Institut für Veterinärphysiologie
der Vetsuisse-Fakultät Universität Zürich

Direktor: Prof. Dr. med. vet. Max Gassmann
Arbeitsgruppe Prof. Dr. med. vet. Thomas A. Lutz

Arbeit unter Leitung von
PD Dr. rer. nat. Thomas Riediger

„Neurotrophic effects of amylin during development of brainstem projections involved in energy homeostasis“

Inaugural-Dissertation

zur Erlangung der Doktorwürde der
Vetsuisse-Fakultät Universität Zürich

vorgelegt von

Andreas Hermann

Tierarzt
von Fläsch, GR

genehmigt auf Antrag von

PD Dr. rer. nat. Thomas Riediger, Referent

Prof. Dr. med. vet. Ulrich Hübscher, Korreferent

Zürich 2009

TABLE OF CONTENT

LIST OF ABBREVIATIONS

AP	area postrema
ARH	arcuate nucleus of the hypothalamus
α-MSH	alpha-melanocyte-stimulating hormone
BBB	blood brain barrier
BST	bed nucleus of the stria terminalis
CCK	cholecystokinin
CeA	central nucleus of amygdala
cGMP	cyclic guanosine monophosphate
CGRP	calcitonin gene-related peptide
CNS	central nervous system
CT	calcitonin
CTR	caltitonin receptor
CVOs	circumventricular organs
DMH	dorsomedial nucleus of the hypothalamus
DMNV	dorsal motor nucleus of the vagus
het	heterozygous
IAPP	islet amyloid polypeptide
IP	intraperitoneal
ko	knockout
LHA	lateral hypothalamic area
NPY	neuropetide Y
NTS	nucleus of the solitary tract
ob/ob mouse	leptin deficient mouse
OVLT	organum vasculosum of the lamina terminalis
PbN	parabrachial nucleus
PCR	Polymerase Chain Reaction
PVH	periventricular nucleus of the hypothalamus
RAMP	receptor activity modifying protein
SFO	subfornical organ
wt	wildtype

1 Introduction

1.1 Energy homeostasis

Energy homeostasis is in balance when energy intake (ingestion and absorption of calories) equals energy output (energy expenditure). Therefore food intake and energy expenditure play critical roles in the maintenance of energy balance. Body mass and composition reflect the collective effects of three processes of energy homeostasis: energy intake, energy storage, and energy expenditure. Excessive energy intake results in storage of energy in fat depots leading to increased body weight and body adiposity.

The central nervous system (CNS) monitors the energy status of the body (energy stores, energy intake and energy expenditure) and modulates both food intake and energy expenditure. This negative feedback control operates to maintain body fat stores more or less constant over long periods of time. The CNS receives inputs from several different signals such as metabolic, neural and endocrine factors.

The control of food intake in humans and animals is a complex and fine-tuned interaction between different hormones, gastrointestinal stimuli, and neurotransmitters. Both peripheral and central feedback signals are processed in the CNS and result in increased food intake (“hunger”) or decreased food intake (“satiation”). A number of parameters are involved in the feedback control of an ongoing meal, among others vision, smell, or taste (Woods, Benoit et al. 2004). These signals are counteracted by signals arising from the stomach and intestine, as e.g. demonstrated in sham feeding experiments with gastric fistula (Davis and Campbell 1973).

Interaction of food with the stomach and intestine elicits the secretion of different gut peptides and other signals which coordinate and optimize the digestive processes. Interestingly, most of these signals also seem to be involved in the control of eating. The first discovered satiation signal is the gut peptide cholecystokinin (CCK) (Gibbs, Young et al. 1973). The size of a meal is dose-dependently reduced after administration of CCK prior to that meal. In addition to CCK, there are other satiation signals which inform the brain precisely about what has been ingested, e.g. gastrin releasing peptide (Stein and Woods 1982), somatostatin (Lotter, Krinsky et al. 1981), glucagon-like peptide-1 (Naslund, Barkeling et al. 1999), apolipoprotein A-IV (Fujimoto, Machidori et al. 1993) and peptide YY

(Batterham, Cowley et al. 2002). All these peptides secreted from the gastrointestinal system have been reported to reduce meal size when administered systemically. In addition to these gastrointestinal peptides, the hormones amylin (Chance, Balasubramaniam et al. 1991; Lutz, Del Prete et al. 1994) and glucagon (Woods, Lutz et al. 2006) secreted from the pancreatic islets during meals, are considered to have similar characteristics.

The mechanism of action by which each of these peptides signals to the CNS and contributes to the phenomenon of satiation may be different. Some are thought either to activate receptors on vagal afferent fibers projecting to the hindbrain, e.g. CCK (Lorenz and Goldman 1982; Davison and Clarke 1988) and glucagon (Geary, Le Sauter et al. 1993; Langhans 1996) or else to stimulate the hindbrain directly at sites with an open blood-brain barrier (BBB) such as amylin acting on the area postrema (Lutz, Del Prete et al. 1995; Lutz, Senn et al. 1998).

The hormones insulin and leptin are considered as important adiposity signals (Schwartz 1997; Woods, Seeley et al. 1998; Schwartz, Woods et al. 2000). Both hormones circulate at levels proportional to body fat content (Bagdade, Bierman et al. 1967; Considine, Sinha et al. 1996), hence reflecting the size of the body adipose tissue. They enter the CNS in proportion to their plasma level (Baura, Foster et al. 1993; Schwartz, Peskind et al. 1996).

Genetically obese mice (*ob/ob* mouse) have been suggested to lack a circulating factor (Ingalls, Dickie et al. 1950). This factor was discovered much later as the gene product of the ob gene and was named leptin (Zhang, Proenca et al. 1994). It is secreted by adipocytes into the bloodstream and reaches the brain, where it influences specific hypothalamic pathways resulting in a reduction in food intake and an increase in energy expenditure. The central target site of leptin is supposed to be the arcuate nucleus (ARH) located in the hypothalamus, where leptin inhibits the release of the orexigenic neuropetide Y and agouti-related protein (Mercer, Hoggard et al. 1996; Guan, Hess et al. 1997; Baskin, Hahn et al. 1999). Leptin also activates proopiomelanocortin neurons to increase the production and release of the anorexigenic hormone α-MSH.

1.2 Amylin

1.2.1 Structure and occurrence

Eugene Opie described in 1901 the occurrence of “hyaline degeneration of the islands of Langerhans” in patients with hyperglycaemia (Opie 1901). He found that the secreting tissue of the gland is destroyed for the most part and is replaced by fibrous dense tissue as a homogeneous material within every islet. This was the first description of islet amyloid. In the middle of the 1980’s the major component of these amyloid deposits confined to the islets of Langerhans was isolated, sequenced and termed islet amyloid polypeptide (IAPP) and later amylin (Westermark, Wernstedt et al. 1986; Cooper, Willis et al. 1987; Westermark, Wernstedt et al. 1987b; Westermark, Wilander et al. 1987c; Leighton and Cooper 1988).
Amylin is now known to be also a physiologically important circulating hormone. It is a 37-amino-acid peptide and is mainly produced in the β-cells of islets of Langerhans in the pancreas (Denijn, De Weger et al. 1992). It is stored in the same secretory granules as insulin (Westermark, Wernstedt et al. 1987a; Westermark, Wernstedt et al. 1987b; Johnson, O'Brien et al. 1988). The co-secretion of amylin from the β-cells together with insulin is induced by nutrient stimuli, e.g. before and during food intake or due to the increase of blood glucose levels (Lukinius, Wilander et al. 1989; Butler, Chou et al. 1990; Moore and Cooper 1991). The ratio of amylin : insulin release ranges between 1-5 : 100 under physiological conditions. The level of the postprandial amylin concentration in the blood depends on the amount of food eaten (Butler, Chou et al. 1990). Apart from the β-cells as the main production site, amylin is also synthesized in lower concentrations in other tissues, namely in the gastrointestinal tract (especially in the antrum pyloricum and colon), in the lung, and in certain parts of the nerve tissue (e.g. spinal ganglia) (Ferrier, Pierson et al. 1989; Asai, Nakazato et al. 1990; Nicholl, Bhatavdekar et al. 1992).

Amylin belongs to the calcitonin gene peptide superfamily consisting of calcitonin (CT), calcitonin gene-related peptide (CGRP), adrenomedullin and has major sequence homology with CGRP. All these peptides are derived from a precursor protein expressed by the CALC1 gene. Aside from the structural homology, they exert similar biological effects and have similar components of receptors (Wimalawansa 1997).
The specificity of the receptors is modulated by so-called receptor activity modifying proteins (RAMP’s) that are co-expressed with the calcitonin receptor (CTR). Co-expression of the

CTR with RAMP1 or RAMP3 leads to a specific amylin receptor (Christopoulos, Perry et al. 1999; Foord and Marshall 1999; Muff, Buhlmann et al. 1999; Sexton, Albiston et al. 2001).

1.2.2 Effects

1.2.2.1 Effects of amylin on nutrient fluxes

In today's view, effects of amylin on nutrient flux complement those of insulin. Amylin controls the nutrient flux from the ingested diet to the blood stream while insulin modulates more the utilisation of nutrients (mainly glucose) out of this reservoir. The best investigated functions of amylin to control nutrient fluxes are its effects to inhibit glucagon secretion and gastric emptying (Fig. 1.)

The prandial glucagon secretion from pancreatic α-cells is inhibited by insulin. *Gedulin, Rink et al.* (1997) showed that amylin also inhibits α-cell secretion of glucagon in response to infused amino acids (L-arginine). Amylin administration dose-dependently suppressed the glucagon response to arginine. The suppression of postprandial glucagon secretion leads to decreased hepatic glucose release (Weyer, Maggs et al. 2001).

A further effect of amylin is an inhibition of gastric emptying that delays the transport of ingesta from the stomach to the small intestine without affecting small bowel or colonic transit (Young, Gedulin et al. 1996; Samsom, Szarka et al. 2000). This suppression of vagus-mediated regulation of gastric emptying was also reported by *Weyer, Maggs et al*. (2001) as an indirect regulation of glucose absorption (Weyer, Maggs et al. 2001), thereby helping to control the influx of endogenous and exogenous glucose, respectively. Additionally, amylin exerts a gastric-protecting effect by an inhibition of both gastric motility (Clementi, Caruso et al. 1996; Kong, King et al. 1997) and secretion of gastric acid.

1.2.2.2 Effects on food intake

Amylin plays a physiological role in the control of eating (Fig. 1.). Its suppressive effect on eating has been demonstrated after peripheral (Chance, Balasubramaniam et al. 1993; Lutz, Del Prete et al. 1994; Morley, Flood et al. 1994; Lutz, Geary et al. 1995) or

central (Balasubramaniam, Renugopalakrishnan et al. 1991; Chance, Balasubramaniam et al. 1991; Chance, Balasubramaniam et al. 1992; Lutz, Rossi et al. 1998c) administration. Amylin's anorectic effect is mainly caused by a reduction in size and duration of the first meal after acute administration (Lutz, Geary et al. 1995) suggesting that amylin inhibits feeding by a meal-ending satiation processes. Similar findings, i.e. that amylin decreases eating mainly by a meal size effect, were obtained after chronic amylin infusion at low doses (Arnelo, Permert et al. 1997; Lutz, Mollet et al. 2001a). The anorectic effect of amylin is considered specific because neither a peripheral nor a central administration of amylin reduce food intake by producing a conditioned taste aversion (Chance, Balasubramaniam et al. 1992; Lutz, Geary et al. 1995; Rushing, Seeley et al. 2002).

To investigate whether amylin acts in the periphery or has a central site of action, experiments were performed using rats with lesioned afferent nerve fibres because abdominal vagal and splanchnic afferents play an important role in the control of food intake by transmission of various signals to the central nervous system. Interestingly, the anorectic effect of amylin was not blocked in animals with a dissection of the common hepatic vagus branch (Lutz, Del Prete et al. 1994) or a destruction of primary sensory (vagal and splanchnic) afferents caused by an intraperitoneal (IP) administration of the neurotoxin capsaicin (Lutz, Althaus et al. 1998b). Hence, contrary to CCK (Joyner, Smith et al. 1993), the anorectic effect of peripherally administered amylin does not depend on an intact abdominal vagus (Lutz, Althaus et al. 1998b). These findings suggest a central site of amylin's action (Morley, Flood et al. 1994; Lutz, Del Prete et al. 1995).

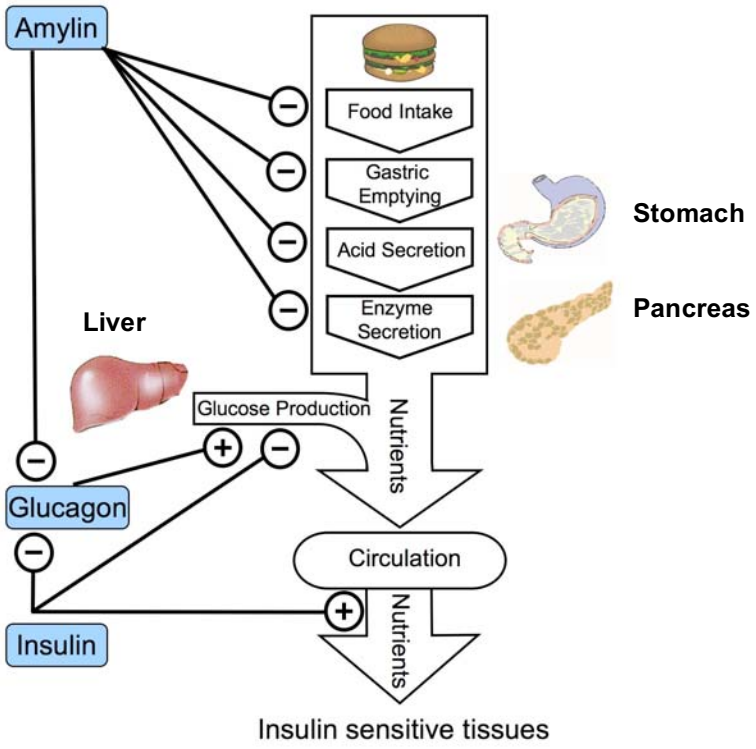

Fig. 1. Effects of amylin (adapted from A. Young, 2005). Amylin is secreted in response to nutrients. The nutrient entry into the circulation is controlled by amylin-mediated inhibition of food intake, nutrient digestion, nutrient transit, and hepatic glucose production (glucagon). All these amylin effects complement the actions of insulin which accelerates nutrient disposal and storage.

There are several indications that amylin may also act as an adiposity signal like leptin and insulin. Interestingly, recent studies showed synergistic effects of amylin and leptin in leptin-resistant, diet-induced obese rats in which amylin agonists restore leptin responsiveness (Roth, Roland et al. 2008). Furthermore the weight loss synergy was specific to amylin treatment, compared with other anorexigenic peptides (e.g. peptide YY or glucagon-like peptide-1). Addition of leptin after 14d amylin pretreatment caused further weight loss, compared to amylin or leptin monotherapy. A long term clinical study in overweight/obese subjects also demonstrated a greater weight loss of co-administration of recombinant human leptin and the amylin analogue pramlintide compared to either treatment alone (Roth, Roland et al. 2008).

These findings provide both nonclinical and clinical evidence that amylin agonism restores leptin responsiveness in diet-induced obesity. Based on these findings amylin is

currently under investigation as a promising pharmacotherapeutical approach to treat obesity and diabetes (Edelman, Maier et al. 2008; Kesty, Roth et al. 2008).

1.3 Area postrema

The actions of amylin on food intake, glucagon secretion and gastric emptying are mediated by the area postrema (AP) a brain structure located in the medulla oblongata (Lutz 2005). The AP as a main site of amylin's effect has some particular properties and is connected to other brain areas which are involved in regulation of food intake and energy homeostasis.

1.3.1 Morphology and function

The AP belongs to the so-called circumventricular organs (CVO's) located around the ventricular system. The CVO's have common morphological and functional characteristics that differentiate them from the rest of the nervous system. A specific property are cellular contacts with two fluid compartments, blood and cerebrospinal fluid (Johnson and Gross 1993). In mammals, there are different CVO's such as the subfornical organ (SFO), organum vasculosum of the lamina terminalis (OVLT), median eminence, subcommissural organ, pineal gland, posterior pituitary, and the AP. Some of them namely the AP, SFO, and the OVLT are supposed to be targets for blood-borne information, e.g. hormones, reaching the brain this way.

Most CVO's are densely vascularized and have a permeable capillary network that allows secretion or tissue penetration by different circulating substances. This differentiates the CVO's from other CNS structures where the permeability of the BBB is limited by the microvascular characteristics of the capillary endothelium (Gross 1992).

The AP, with its v-shaped appearance, is situated on the dorsal surface of the medulla oblongata adjacent to the nucleus of the solitary tract (NTS) and located at the caudal end of the fourth ventricle. It was one of the first recognized structures of the CVO's with a lacking BBB where circulating substances have direct access to neurons via the fenestrated capillaries. One of the first functions described for the AP was its role as "chemoreceptor trigger zone" (Borison 1974; Carpenter 1990) provoking emesis as a protection reflex that

allows an individual to rid itself of ingested toxins or poisons. Studies using animals with lesions in the AP demonstrated that the AP is involved in developing a conditioned taste aversion e.g. due to the treatment with different aversive stimuli (Ritter, McGlone et al. 1980).

The AP plays an important role in the control of feeding behaviour (Fry and Ferguson 2007) as also demonstrated in AP lesioned animals (Edwards and Ritter 1981; Hyde and Miselis 1983). In the context of the present study, it is important to note that the AP was identified as primary receptive target area for amylin. Binding sites with high affinity for amylin have been discovered in different brain structures, but particularly the AP contains a high density of amylin receptors (Bhogal, Smith et al. 1992; Beaumont, Kenney et al. 1993; Sexton, Paxinos et al. 1994; Christopoulos, Paxinos et al. 1995). After a thermal ablation of the AP/NTS, the anorectic effect of IP injected amylin (5 microg/kg) was significantly reduced in food deprived rats (Lutz, Senn et al. 1998a). Furthermore, infusion of various doses of amylin with chronic cannulas aiming at the AP inhibited food intake for about 2h after food presentation. Infusion of the amylin antagonist AC187 into the AP reduced the anorectic effect induced by an IP injection of amylin, and AC187 alone increased food intake when administered into the AP.

An action of amylin on AP neurons was also characterized by the detection of c-Fos expression. c-Fos is an immediate early gene product that is used as an experimental marker of neuronal cell activation. The expression of c-Fos is induced by activation of neurons following specific stimuli and is assessed by immunohistochemical techniques (Hoffman, Smith et al. 1993). In several studies Fos-like immunoreactivity was used to investigate the amylin-mediated activation of neurons e.g. in the AP (Rowland, Crews et al. 1997; Riediger, Schmid et al. 2001). Peripheral administration of amylin induced c-Fos expression in the AP, the nucleus of the solitary tract, the bed nucleus of the stria terminalis (BST) and the central nucleus of the amygdala (CeA). Further evidence for an activation of AP neurons was provided by electrophysiological studies with in vitro slice preparations of the rat AP. Amylin induced dose-dependent excitatory responses in these neurons, which could be antagonized by the amylin receptor blocker AC187 (Riediger, Schmid et al. 2001). This excitatory action of amylin in the AP appears to be mediated by the excitatory second messenger cGMP (Riediger, Schmid et al. 2001).

1.3.2 Neuronal connections of the AP

The projections of the AP are predominantly efferent comprising 3 different functional groups. A first group of AP projections which are most relevant in the context of the present study have their termination field in the NTS and the parabrachial nucleus (PbN) as brain structures recognized to relay afferent visceral and gustatory information. Thus the AP is able to modulate enteroceptive signals of the periphery (van der Kooy and Koda 1983; Shapiro and Miselis 1985; Johnson and Gross 1993). These target structures are strongly interconnected with other nuclei located in more rostral brain areas including the CeA, BST and hypothalamic centers, amongst others the lateral hypothalamic area (LHA), formerly recognized as “hunger center” (Ricardo and Koh 1978; van der Kooy, Koda et al. 1984).

The second group of efferent connections project to catecholaminergic cells of the dorsolateral tegmentum system. Both ascending and descending projections to cortical limbic and hypothalamic centers and intermediolateral sympathetic neurons of the spinal cord, respectively, are influenced by these projections. The last group of efferent projections connects the AP with the dorsal motor nucleus of the vagus (DMNV) and the nucleus ambiguous. These connections modulate the parasympathetic outflow of these nuclei to the viscera.

Apart from efferent connections to several brain structures like the NTS and the PbN, the AP also receives neuronal afferents from these centers. Additionally the AP receives projections from hypothalamic nuclei as the major central afferent input to the AP, e.g. from the paraventricular (PVH) and dorsomedial (DMH) hypothalamic nuclei, and the perifornicular region (Shapiro and Miselis 1985).

In summary the AP holds a unique position to receive and modulate ascending and descending information and to interconnect different signals from various structures of the brain and the periphery.

1.4 Neurotrophic effects

The development of the rodent brain is not completed at the time of birth and certain circulating hormones, e.g. sex hormones, influence brain development and the formation of different central pathways (Rhees, Shryne et al. 1990; Ibanez, Gu et al. 2001). Various studies implied that hormones involved in the control of food intake and energy homeostasis may also exert neurotrophic effects in the developing brain.

Ghrelin, a 28 amino acid gastric peptide hormone, regulates the secretion of growth hormone and plays a role as an orexigenic signal in controlling feeding behaviour and energy homeostasis. In rats ghrelin stimulates food intake, induces adiposity, and increases body weight (Tschop, Smiley et al. 2000; Wren, Small et al. 2000). Ghrelin acts directly on neurones of the DMNV (Zhang, Lin et al. 2004) and neurones of the NTS (Zhang, Hu et al. 2005) to stimulate neurogenesis both in vivo and in vitro.

Leptin has been supposed to have important trophic actions on neurons in the CNS. As mentioned above, the ARH is a major site of leptin's actions on feeding and energy balance. Leptin has direct access to the hypothalamic neurons via the ARH (Sawchenko 1998; Elmquist, Elias et al. 1999) and cells of the ARH express leptin receptors (Fei, Okano et al. 1997; Elmquist, Bjorbaek et al. 1998). Projections to other hypothalamic nuclei such as the PVH and DMH, as well as the LHA belong to the hypothalamic neurocircuitry involved in leptin signalling.

Although it has been shown that leptin receptors are also expressed in the brain of foetal and neonatal rats and mice (Matsuda, Yokota et al. 1999; Udagawa, Hatta et al. 2000), the neonatal brain is only marginally susceptive to leptin's action (Mistry, Swick et al. 1999). In contrast to leptin's effects in adults, leptin is unable to inhibit growth, food intake, or energy expenditure during the postnatal period (Mistry, Swick et al. 1999; Ahima and Hileman 2000; Proulx, Richard et al. 2002). Interestingly, postnatal plasma leptin levels are markedly elevated in the second week of life and decline to adult values around weaning (Devaskar, Ollesch et al. 1997; Ahima, Prabakaran et al. 1998). A possible role for the occurrence of this neonatal leptin surge has been supposed to be that of an important developmental neurotrophic signal. *Steppan et al.* (1999) demonstrated that brains of *ob/ob* mice, i.e. mice which lack leptin production, are smaller in weight and cortical volume (Steppan and Swick 1999). Furthermore a daily IP injection of leptin for 2 weeks to 4-week-old *ob/ob* mice caused an increased brain weight and appeared to be partially a result of increased cell number. Besides the decreased brain weight in leptin deficient mice, an

immature expression pattern of synaptic and glial proteins as neuronal and glial markers was observed. After six weeks of leptin treatment, both brain weight and protein content were increased (Ahima, Bjorbaek et al. 1999).

Important evidence for leptin's role in brain development was provided by studies using DiI axonal labelling. *Bouret et al.* (2004a) demonstrated that ARH projections to the hypothalamic paraventricular nucleus are immature at birth and develop mainly during the second week of life (Bouret, Draper et al. 2004a). The development of these ARH projections after birth coincides with the naturally occurring surge of leptin during this time period. Interestingly, the neuronal projection pathways from the ARH to the PVH are severely underdeveloped in leptin-deficient *ob/ob* mice. Treatment of adult mice with leptin does not recover these neuroanatomical defects (Bouret, Draper et al. 2004b) but daily treatment of *ob/ob* neonates with leptin from P4 to P12 rescues the development of these ARH projections. In line with this finding, leptin promotes neurite outgrowth from ARH neurons in vitro (Bouret, Draper et al. 2004b). Hence, leptin plays an important role as neurotrophic factor during the development of the rodent hypothalamus and this activity is confined to a critical period after birth (Bouret and Simerly 2004c; Bouret and Simerly 2006; Bouret and Simerly 2007).

1.5 Amylin knockout mice

Amylin-deficient mice used in this study have been created to investigate the physiological role of amylin and the consequences of a lack of endogenous amylin. Generation of amylin-deficienct mice has been described previously by *Gebre-Medhin et al*., (1998a) (see chapter 2.1.1.1).

The mouse amylin gene is located on chromosome 6 and consists of three exons encoding preproamylin (Ekawa, Nishi et al. 1997). Exon 3 was targeted to generate amylin knockout mice (Gebre-Medhin, Mulder et al. 1998a; Gebre-Medhin, Mulder et al. 1998b; Mulder, Gebre-Medhin et al. 2000; Carlsson, Karlsson et al. 2002). Amylin deficient mice ($IAPP^{-/-}$) are phenotypically healthy and are born according to Mendelian frequencies when bred in transgenic colinies (Gebre-Medhin, Mulder et al. 1998b; Muff, Born et al. 2004). They have normal basal plasma insulin and glucose levels, gonadal fat pad weight, islet weight, blood pressure, and blood perfusion of islets (Gebre-Medhin, Mulder et al. 1998b; Carlsson, Karlsson et al. 2002). Concerning the bone metabolism, $IAPP^{-/-}$ mice have low bone

mass with decreased cortical and trabecular thickness and connectivity (Dacquin, Davey et al. 2004).

Amylin knockout mice have also been used to study the physiological role of amylin in the control of food intake and body weight (Lutz 2006). A comparison of body weight of 5 months old mice demonstrated no difference between knockout and wildtype animals but IAPP$^{-/-}$ mice showed a higher rate of body weight gain compared with corresponding wildtype controls. Food intake was slightly but non-significantly higher in amylin IAPP$^{-/-}$ mice than in control animals (Mollet, Meier et al. 2003; Lutz 2005).

1.6 Aim of the study

Apart from various effects on food intake and energy homeostasis (see chapter 1.2.2), amylin has been shown to play a role in developmental processes in the immature rodent organism. Amylin is already expressed in the foetal period suggesting an effect as growth factor at this developmental stage (Rindi, Terenghi et al. 1991; Mulder, Ekelund et al. 1997). Trophic effects of amylin have been described in different tissues. Amylin stimulates osteoblast proliferation (Cornish, Callon et al. 1995) and osteoclast differentation (Cornish, Callon et al. 2001), and it plays an important role as a growth factor in kidney development (Harris, Cooper et al. 1997; Wookey, Tikellis et al. 1998). Furthermore amylin's trophic effect has also been demonstrated in isolated foetal pancreatic cells suggesting a potential role as regulator of proliferation in neonatal pancreatic islet (Karlsson and Sandler 2001). Up to now, there are no studies investigating trophic effects of amylin in the CNS.

Based on a similar approach replicating the experiments on leptin's role in the development of the hypothalamic neuro-circuits involved in the control of eating, we used DiI axonal labelling in amylin deficient mice to investigate whether amylin may also function as a neurotrophic factor in the hindbrain. We established a neuronal tracing technique to analyse the development of projections connecting the AP to the NTS.

We expected that amylin may participate in the development of efferent neuronal projections originating from the AP and projecting to the NTS, hence in principle similar to what has been shown for leptin's neurotrophic effect in the hypothalamus. Thus, we hypothesised that IAPP$^{-/-}$ mice have a reduced fiber density in the NTS compared to wildtype littermate animals.

We wanted to answer the following questions:

- Does amylin contribute to the development of neuronal projections originating in the AP by exerting a neurotrophic effect? Is amylin deficiency associated with a reduced density of neuronal fibers in the AP/NTS region?

- Does the neurotrophic effect of amylin on the development of neuronal projections differ at various timepoints in the postnatal period?

- Does the neurotrophic effect of amylin on development of neuronal projections differ between male and female animals?

- Are postnatal plasma amylin levels in wildtype mice similar to or even higher than amylin concentrations in adult animals? The latter could be indicative of amylin being a neurotrophic signal during the early developmental stage.

2 Animals, materials, methods

2.1 Animals and housing

2.1.1 Animals

2.1.1.1 Generation of amylin knockout mice

Generation of amylin-deficient mice has been described previously by *Gebre-Medhin et al.,* (1998b). Briefly, $IAPP^{-/-}$ mice were created by cloning a 10.5-kbp fragment containing the murine IAPP gene from a genomic mouse Balb/c library (Stratagene) by plaque hybridization to the human amylin cDNA. An 890bp SphI/BamHI fragment containing part of exon 3, and internal to a 3.46kbp HindIII/XbaI fragment, was replaced by a phosphoglycerate kinase (PGK) promoter-driven neomycin resistance gene (neo)-selection cassette (Fig. 2.). This resulted in the deletion of all sequence encoding the 37-amino-acid IAPP peptide. The resulting DNA construct was fused with a 5.1kbp XbaI/SalI fragment. Mouse 129Ola/sv embryonic stem cells were cultured and transfected, screened for recombinant ES cell clones, and therefore chimeric mice were generated.

The screening probe was a 1.5kbp EcoRI-HindIII genomic DNA fragment which contained the second exon of the IAPP gene. The deletion of the IAPP coding sequence in the targeted IAPP allele was confirmed using exon 3-specific oligonucleotide probes bp 89-179 and bp 170-253 of the mouse IAPP sequence. These probes were radio labelled using 5' GTTGCTGGAA3' and 5'CCTAGGGGAC3', respectively, as primers in the presence of dCTP, unlabelled dATP, dTTP, and dGTP and the Klenow fragment of DNA polymerase I. Hybridizations were carried out at high stringency.

For our studies, we did not generate the knockout mice ourselves, but our breeders were supplied by *Amylin Pharmaceuticals, Inc.,* USA (see 2.1.1.2).

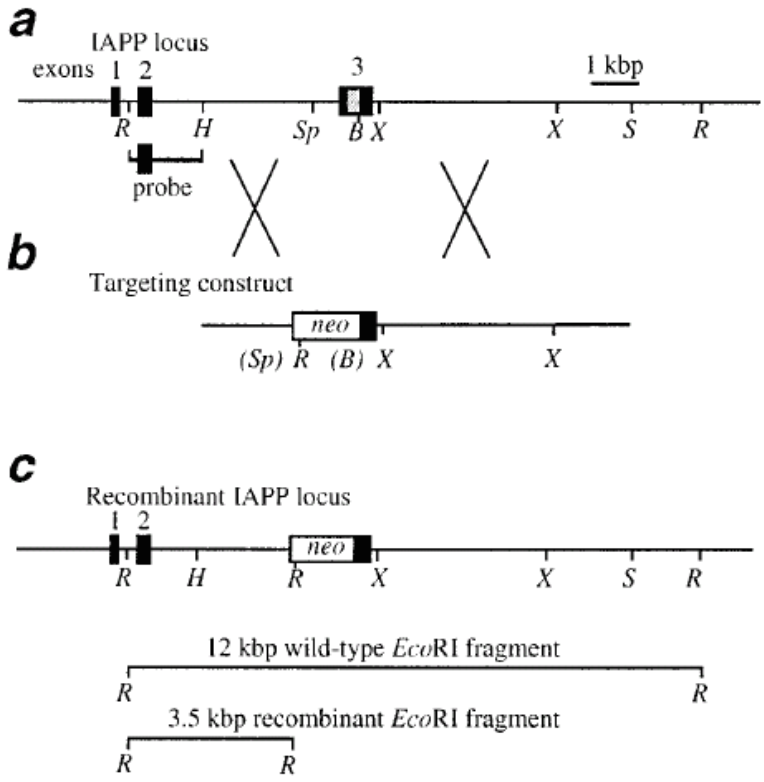

Fig. 2. IAPP gene-targeting strategy (adapted from Gebre-Medhin et al., 1998b) **a)** Schematic map of the murine IAPP locus with the sequence coding for mature IAPP boxed in the third exon, and the screening probe containing exon 2. **b)** The targeting construct designed to replace the IAPP coding sequence present in exon 3 with a neomycin-resistance gene (*neo*)-selection marker. **c)** The IAPP locus following homologous recombination. The screening probe detects the wildtype IAPP locus as a 12kbp *Eco*RI DNA restriction fragment, while the recombinant IAPP locus is detected as a 3.5kbp *Eco*RI fragment. *R, Eco*RI; *B, Bam*HI; *H, Hind*III; *S, Sal*I; *Sp, Sph*I; *X, Xba*I.

2.1.1.2 Animal breeding

For the present studies it was important to use $IAPP^{-/-}$ and $IAPP^{+/+}$ littermates in order to minimize all prenatal developmental influences unrelated to amylin deficiency. Therefore heterozygous breeding pairs ($IAPP^{+/-}$) were generated. Homozygous amylin knockout mice were obtained from *Amylin Pharmaceuticals, Inc.,* USA. As shown in Figure 3 the transgenic mice were crossbred with C57BL/6 wildtype mice (Jackson Laboratories, USA) to generate heterozygous animals (F1). Breeding pairs from the heterozygous F1 generation were used to generate F2 animals. According to the Mendelian inheritance, F2 animals were expected to

comprise 25% BL/6 homozygous IAPP$^{+/+}$ *wildtype (wt)*, 50% *heterozygous* (*het)* IAPP$^{+/-}$ and 25% IAPP$^{-/-}$ *knockout (ko)* mice (ratio of 1:2:1).

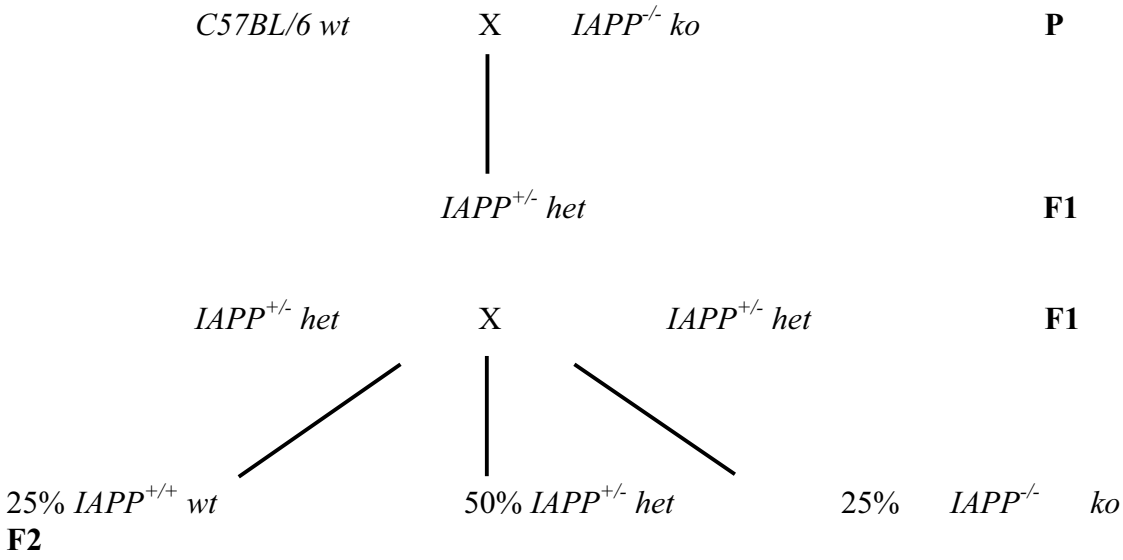

Fig. 3. Breeding of the transgenic mice. Expected distribution of genotypes in the F2 generation. IAPP$^{-/-}$ breeders were obtained from *Amylin Pharmaceuticals, Inc.,* USA, C57/BL6 breeders were obtained from *Jackson Laboratories,* USA.

For DiI-labelling experiments, male and female IAPP$^{-/-}$ mice and their IAPP$^{+/+}$ littermates were used on day 10 and 14 after birth (P10, P14), respectively, to compare the density of the projection neurons from the AP to the NTS. Wildtype BL/6 mice (P6 to P9) were used to measure the postnatal plasma amylin levels. Experiments were in accordance with the guidelines of the Veterinary Office of the Canton Zurich, Switzerland.

All animals were kept in standard macrolon cages until they were used for the experiments. The breeding pairs had *ad libitum* access to food (standard pellet chow, #3430, Kliba Nafag AG, Gossau, Switzerland) and water. The litters were housed in the same cages as their parents. Animals were kept under an artificial 12:12h light/dark cycle (lights off 18.00h).

2.2 DiI fiber labelling

2.2.1 Tissue fixation, perfusion

2.2.1.1 Material

1. Micro eye scissor (85mm, 3 3/8", B. Braun Medical AG, Tuttlingen, Germany)
2. Micro forceps (Jeweler Type, 0,3mm, angled, 110mm, 4 3/8", B. Braun Medical AG)
3. Canulae to fix extremity (Terumo, 26G x ½ “, Leuven, Belgium)
4. Three-way stopcock (B. Braun Medical AG) with flexible tubes
5. Clamp to fix perfusion canula in the left ventricle
6. 1ml syringes (Omnifix 1ml, Braun Melsungen AG, Melsungen, Germany)
7. Canulae (Terumo, 26G x ½ “, Leuven, Belgium)
8. 4% paraformaldehyde in sodium phosphat buffer (pH = 7.4)
    a. Paraformaldehyde purum, ≥95.0% (Sigma-Aldrich, Saint Louis MO, USA)
    b. Stock solution I (Tab. 1.)
    c. Stock solution II (Tab. 1.)
9. 0.9% NaCl
10. Tribromoethanol (0.15 - 0.2ml for P7 - P14 pups) (Tab. 2.)
    a. Stock solution:
        - 2,2,2-Tribromoethanol (Aldrich Chemical, St. Louis, MO. USA)
        - Ter-amyl alcohol-gold label reagent (Aldrich Chemical)
    b. Working solution:
        - TB EtOH
        - 100% EtOH
        - 0.7% saline

Table 1. Reagents for perfusion

Stock solution	Substance	Concentration [g/l]	End concentration in PB [M]
I	$NaH_2PO_4 \cdot H_2O$	27.6	0.2
II	$Na_2HPO_4 \cdot 2H_2O$	35.85	0.2
0.9% NaCl	NaCl	9	0.15
Preparation of working solution: 500ml ddH2O + 40g paraformaldehyde + 2 pellets of NaOH (approx. 370mg) were stired and heated. Solution was filtered into 115ml of Stock solution I + 385ml of Stock solution II. Finally the pH value was adjusted to 7.4 using HCl.			

Table 2. Tribromoethanol

Solution	Preparation
Stock solution	100g 2,2,2-Tribromoethanol dissolved in 62.5ml of Ter-amyl alcohol-gold label reagent (Kantonsapotheke Zürich KAZ)
Working solution	2ml TB EtOH + 8ml 100% EtOH + 90ml 0.7% saline

2.2.1.2 Method

Anaesthesia

Animals were deeply anesthetised with intraperitoneally injected tribromoethanol (dose = 0.15 - 0.2ml for P7 - P14 pups). The injection site was slightly paramedian between teats and knee flexure and the needle penetrated at an angle in direction to craniomedial. Tribromoethanol was used instead of pentobarbituric acid because it induces anesthesia rapidly and provides good surgical analgesia for approximately one hour. It produces a high degree of surgical tolerance and a strong anaesthetic depth. Moreover its analgetic properties are stronger compared to pentobarbituric acid whereas its depressive effect of the respiratory system is lower. All these factors are critical for anaesthesia of neonatal mouse pups. Anaesthetic depth was confirmed by testing the loss of the flexor reflex of the hind leg with a forceps.

Transcardial perfusion

As soon as the anaesthesia was deep enough, the four legs were fixed with canulae to keep the animal in supine position. After dissecting the skin, the abdomen was opened at the level of the xiphoid process avoiding cutting the liver. The diaphragm was cut through and the thoracic cavity was opened by transecting the costal arches. The heart was carefully exposed and the pericardium was removed. After cutting the ventral part of the left ventricle, a blunt canula-needle was inserted into the incision without reaching the aorta. The needle was fixed with a mini-clamp. The right atrium was then cut with a micro eye scissor before the infusion of a 0.9% NaCl solution into the left ventricle with a hydrostatic pressure of about 150cm for approximately 2 minutes. After exsanguination the three-way stopcock was turned to infuse the ice-cold paraformaldehyde solution for approximately 6-7 minutes.

After perfusion animals were decapitated and the skullcap was carefully exposed. The brains were quickly removed and post fixed in the same 4% paraformaldehyde solution at 4°C for about 10 days until further processing.

2.2.2 DiI implantation

2.2.2.1 Material

1. DiI C_{18} (1,1'-dioctadecyl-3,3,3',3'-tetramethyl-indocarbocyanine perchlorate, Molecular Probes, Eugene, OR), carbocyanine dye used for tracing
2. Micrometer benchmark (100 x 0.01mm, Pyser-SGI Limited, Kent, UK)
3. Insect pin (Minutien, 0.1mm, Bauer Handels GmbH, Adetswil, Switzerland)
4. Zoom stereomicroscope (Wild M8, Leica Microsystems, Nussloch, Germany)
5. Methylene blue for visualization of morphological features of brains during DiI implantation
6. 3 way micromanipulator (SD Instruments, Grants Pass, OR, USA)
7. Dual arm fiber optic illuminator (Intralux® 4000, Volpi AG, Schlieren, Switzerland)

2.2.2.2 Method of implantation

The cerebellum was carefully removed under a stereomicroscope (see Fig. 4.A) to expose the area postrema (AP). To visualize morphological features of the exposed surface, methylene blue was used to identify structures of the medulla oblongata. An insect pin was used to implant a small crystal (~10µm diameter) of the lipophilic tracer DiI into the AP. Before implantation, each DiI-crystal was first checked for uniform size and shape using a micrometer benchmark under the zoom stereomicroscope. The crystals used for implantation had a round shape and a diameter of approximately 10µm.

Under visual guidance and using a micromanipulator, the DiI crystal was first placed on the surface of the AP at the desired implantation site without penetrating the tissue. Afterwards it was pushed into the tissue slightly under the surface with the insect pin. The implantation site was in the center of the horizontal AP surface area (see Fig. 4. + 5.). After implantation, brains were stored in glass vials in a 4% paraformaldehyde solution. The DiI tracer was allowed to migrate for 10 days in the dark at 37°C.

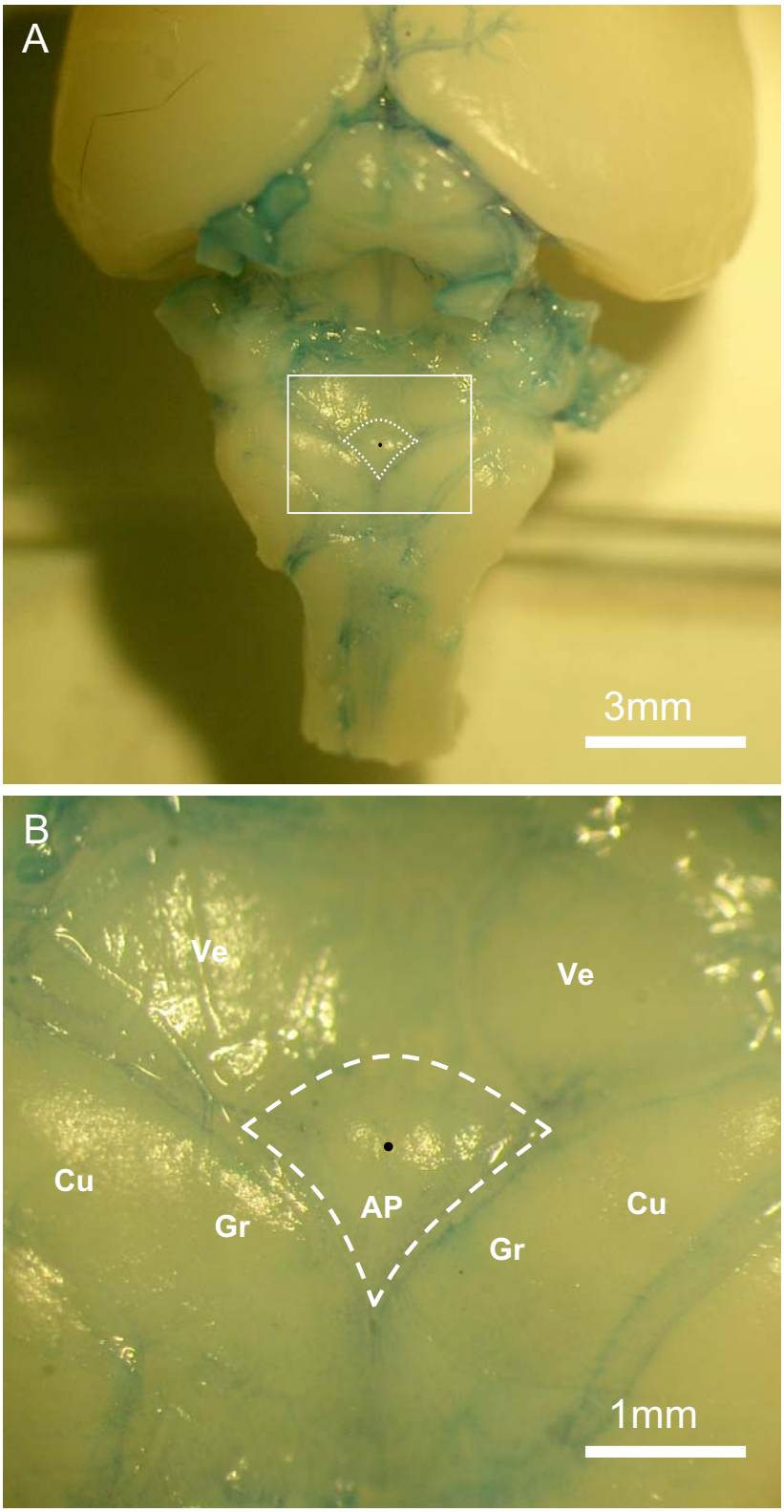

Fig. 4. Surface-area of the AP and implantation site of the DiI crystal

A. Borderline of the AP showed as dotted line

B. Detail enlargement of A (white box); the black dot indicates the implantation site

AP = area postrema, Cu = cuneate nucleus, Gr = gracile nucleus, Ve = vestibular nucleus

2.2.3 Brain slicing

2.2.3.1 Material

1. Vibratome (Leica VT 1000s, Leica Microsystems)
2. Agarose (agarose electrophoresis grade, #820723, MP Biomedicals, Inc., Solon, Ohio, USA)
3. KPBS buffer (0.02M) (Tab. 3.)
4. Multi-well plate (24 Well)
5. Paint brush
6. Poly-L-lysine-coated (Sigma-Aldrich, Inc.) glass slides (Thermo Scienctific, microscope slides 76 x 26mm, Menzel GmbH & Co. KG, Braunschweig, Germany)
7. 65% KPBS buffered glycerol
8. Microscopic cover slips (24 x 50mm, Menzel GmbH & Co. KG)
9. Rapid mounting medium (Entellan®, Merck, Darmstadt, Germany)

Table 3. Composition of KPBS buffer (0.02M)

Substance	Weight [g]	
KH_2PO_4	9.7	Dissolved in 20.58l H_2O to final concentration of 0.02M
K_2HPO_4	56.6	
NaCl	178.2	

2.2.3.2 Preparation of brain slices

After the 10 day incubation period, brains were embedded in 3% agarose. The brains were transected at the mid rostrocaudal level to facilitate embedding in an upright position along the longitudinal axis. The agarose blocks were trimmed and fixed with super glue. 80µm thick coronal sections were cut through the brainstem using a vibratome. The brains were cut approximately between *bregma* -7.08mm to -8.24mm (see Fig. 5., *bregma* levels corresponding to adult mice). The slices were collected with a soft paint brush and kept in KPBS before mounting onto poly-L-lysine-coated glass slides and coverslipped with 65%

KPBS buffered glycerol. Coverslips were finally sealed with rapid mounting medium and the slices were stored at 4°C in the dark.

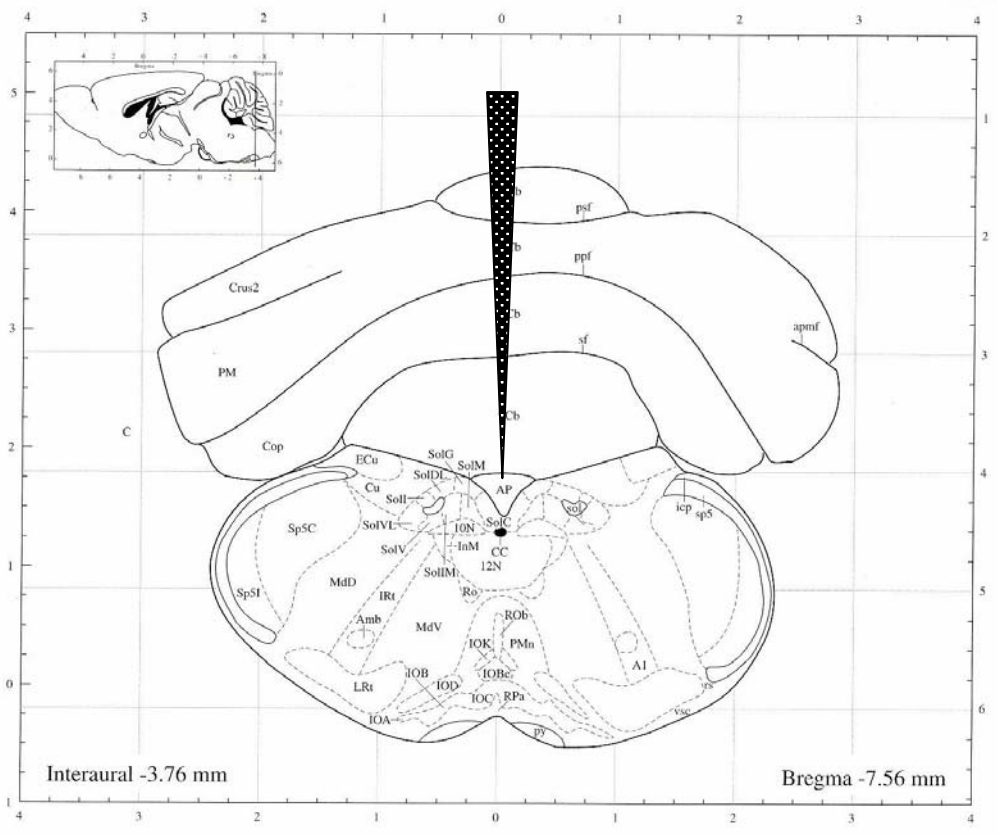

Fig. 5. Coronal diagramm of the brainstem illustrating DiI implantation site in the AP (adapted from Paxinos and Franklin, 2004; image and specifications corresponding to adult mice)

The DiI crystal was implanted slightly under the surface in the center of the horizontal surface area of the AP (tip of the triangle).

2.2.4 Microscopy

2.2.4.1 Fluorescence microscopy

Material

1. Fluorescence microscope (Zeiss Axioskop 2, upright epifluorescence microscope, Zeiss Co., Oberkochen, Germany)
2. Fluorescence filter set 43 (Zeiss Co.; excitation BP 545/25nm, emission BP 605/70nm, Fig. 7.), optimized for DiI dye (excitation/emission, 551/565nm, Fig. 6.)
3. Microscopy digital camera (AxioCam HS, Zeiss Co.)

Method

Sections were evaluated with both conventional fluorescence and confocal microscopy (see 2.2.4.2). The accuracy of the crystal implantation was a precondition for a correct evaluation of all following analyses. Therefore, the success of the crystal implantation was confirmed with the fluorescence microscope equipped with optics for visualization of DiI fluorescence (Fluorescence Filter set 43, Zeiss Co.). Figures 6 + 7 show the spectral range of excitation and emission spectra of DiI dye and the Filterset 43. A crystal implantation was considered successful when the following criteria were met:

- Implantation of crystal
  It was first checked, if the crystal was really implanted into the AP because it could have been implanted too superficially and get lost during processing.

- Symmetry of implantation
  The crystal had to be implanted exactly in the middle of the AP to achieve a symmetric diffusion area. As a consequence, the tracer is able to migrate and distribute uniformly. This was a precondition for a comparable specific labelling.

- Restricted tracer diffusion area

  The unspecific tracer signal caused by diffusion of the tracer around the implantation site had to be restricted to the AP.

- Distribution and extent of fibers (AP, NTS)

  The distribution and extent of fibers in the AP and through the NTS were roughly evaluated in the fluorescence microscope. In case of an unusual distribution (e.g. asymmetric distribution pattern) or if the tissue was damaged, the animals were not included in further evaluation.

For the documentation of the implantation site pictures were taken with a digital camera in different magnifications and section planes.

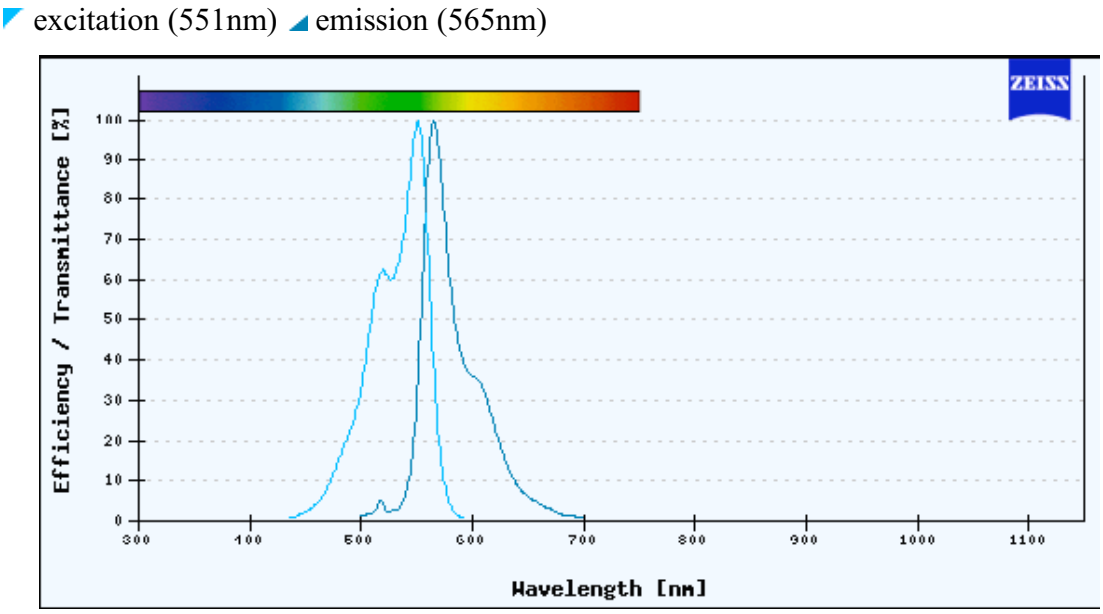

Fig. 6. Spectral range of dye DiI (adapted from Zeiss Co., Germany)

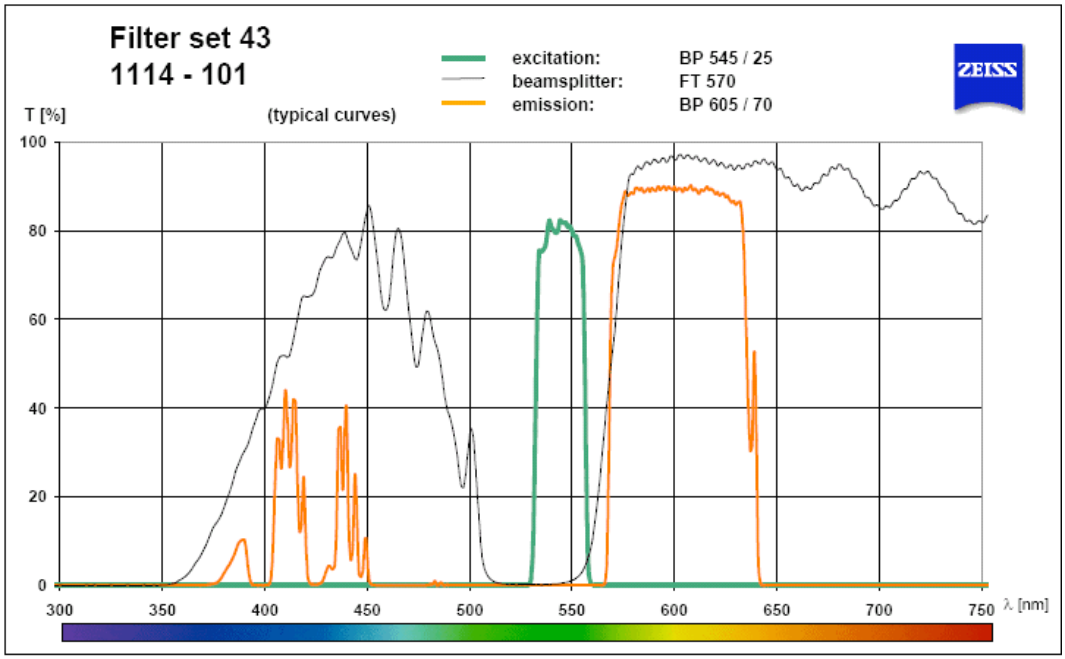

Fig. 7. Spectral range of filterset 43 (adapted from Zeiss Co., Germany)

2.2.4.2 Confocal laser microscopy

Equipment and material

1. Confocal laser-scanning microscope (Leica SP2 AOBS, Leica Microsystems, Wetzlar, Germany)
2. 63x glycerol objective (Leica, HCX PL APO lbd. BL 63x 1.4 CORR)
3. 20x multi objective (Leica, HC PL APO lbd. BL 20x 0.7 IMM / CORR)

Images of DiI-labeled fibers were collected through the NTS region (Fig. 8., white rectangle) by using a confocal laser-scanning microscope. Within each tissue section the NTS region was analysed with a 63x glycerol objective to detect projections from the AP to the NTS. Furthermore a 20x multi objective was used to acquire overview images. The image stacks were collected with a pinhole setting of Airy 1 (232.43µm) and a step length of 0.8µm.

The following settings of the confocal laser-scanning microscope were used to analyse representative sections:

- Laser: 543nm excitation
- Airy 1 pinhole: 232.43µm
- Scan Averaging 6
- Series: The z-Axis interval was adjusted by scanning a 60µm thick bloc with a 0.8µm step length
- Gain, Offset manually adjusted

Confocal microscope settings were adjusted to optimize the signal : noise ratio. A single image stack comprised 75 images with a thickness of 0.8µm each, i.e. a total of 60µm.

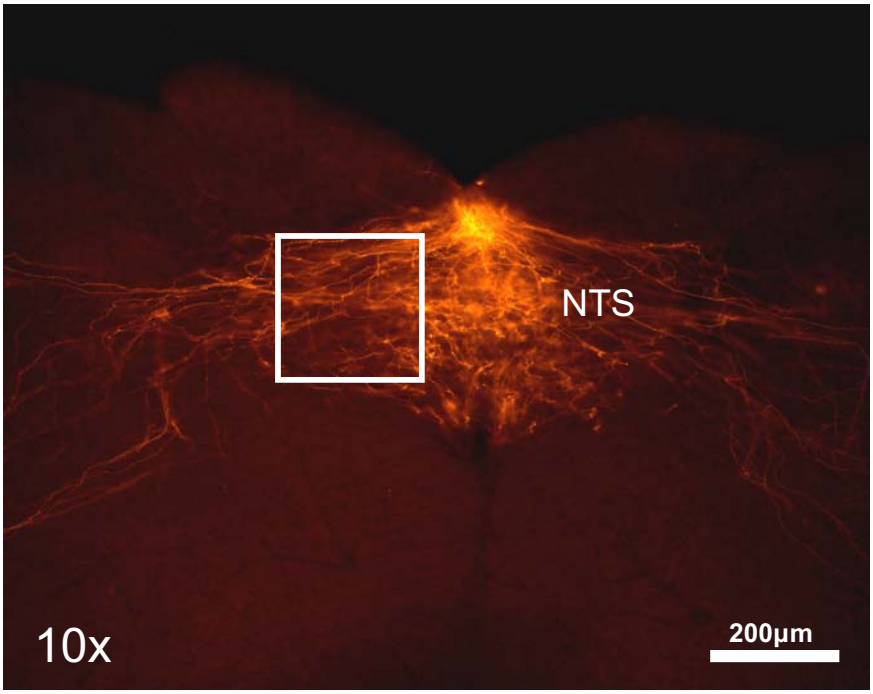

Fig. 8. Fluorescence microscopic image illustrating confocal scanning area in the NTS (white rectangle); *NTS = nucleus of the solitary tract*

2.2.5 Quantitative analysis

Image analysis (three-dimensional reconstruction, volume and surface rendering) was performed using image analysis software (Imaris Vers 6.0.1, Bitplane, Zurich, Switzerland). After importing the image stacks of optical sections into the analysis application, a filament tracer software module with an autopath algorithm was used to calculate the total fiber length contained in the entire volume of the image stack ($3.4 \times 10^{-3} mm^3$). This algorithm generates a filament by connecting start- and endpoints based on local intensity contrast. The signal range of the start- and endpoints was manually set by a thresholding procedure. Afterwards, fibers were skeletonized to a diameter of 1 pixel. The software calculated different parameters of the digitalized fiber skeleton from which the total fiber length in the entire image stack was used for the evaluation.

2.3 Postnatal plasma amylin levels

2.3.1 Blood samples

Material

1. EDTA tripotassium salt blood collection tube (Microvette® 200 K3E, Sarstedt AG, Sevelen, Switzerland)
2. Aprotinin (Protease inhibitor, Labodia SA, Yens, Switzerland)
3. Canulae (Terumo, 26G x ½ “)

Method

To measure the postnatal plasma amylin levels, blood samples from BL/6 wildtype mice were taken at different time points (P6 - P9) after birth. Mouse pups were anesthetised with an IP Injection of Tribromoethanol (0.15 - 0.2ml for P6-P9 pups). After checking the loss of flexor reflexes, the abdomen and the thorax were opened and the heart was carefully exposed. The pericardium was removed before the right ventricle was penetrated with a canula that was attached to a pipette tip. This method had several advantages such as holding

the needle in proper position. Furthermore the blood could be taken easily with one hand and easier than with a normal syringe. The experiment was terminal for the animals.

Blood was immediately transferred into EDTA tubes. The protease inhibitor aprotinin was added instantly. Blood was cooled on ice until centrifugation. An approximate amount of 100µl (P6) - 200µl (P9) of blood per animal was obtained. Samples were centrifuged immediately for 10min at 2800rpm to separate blood plasma. Plasma was subsequently transferred into Eppendorf tubes and stored at -20°C until further processing.

2.3.2 Immunoassay for plasma amylin levels

Material

1. Mouse Endocrine LINCOplex™ KIT - 96 well plate assay (Linco Research, Inc. St Charles Missouri, USA)
2. Luminex Sheath Fluid
3. Sonicator
4. Titer plate shaker
5. Vacuum pump for vacuum filtration
6. Luminex 100 analyzer (Luminex Corp., Austin, TX, USA)

Method

For the analysis of plasma samples, the Mouse Endocrine LINCOplex™ assay, a multianalyte detection system, was conducted according to the manufacturer's instructions (Linco Research, Inc.). Briefly, the assay is based on conventional sandwich assay technology and permits simultaneous detection of multiple hormones from a single sample. The antibody specific for the hormone of interest is covalently coupled to Luminex microspheres uniquely labelled with a fluorescent dye.

The microspheres were incubated with standards, controls, and the plasma samples (10µl) in a 96-well microtiter filter plate with agitation on a plate shaker overnight (17 hours) at 2-8°C. After incubation, the plate was washed 3 times with an assay wash buffer (200µl/well) to remove excess reagents (by vacuum between each washing step) prior to the addition of the detection antibody (50µl/well). After 60min incubation on a plate shaker at

room temperature, 50µl streptavidin-phycoerythrin was added to each well containing 50µl of detection antibody cocktail, and incubated for an additional 30min.

After a final washing step (3 times washing and removing fluids by vacuum filtration), the beads were resuspended in buffer (100µl of Sheath Fluid) and the plate was analyzed using the Luminex 100 analyzer to determine the concentration of the hormones of interest (Precision for amylin: Intra-assay 3.8 – 10.6%, Inter-assay 4.8 – 20.7%, Accuracy: 80.2%).

2.4 Genotyping of IAPP- ko and wildtype mice with PCR

In the present study $IAPP^{-/-}$ mice and their wildtype littermates were used. All animals were generated from heterozygous breeding pairs. Since the genotype of the newborn mouse pups was not known at the time of DiI implantation, all animals had to be genotyped in retrospect. The genotyping was partly conducted externally via a molecular diagnostics company (Transnetyx, Memphis, TN, USA). The genotyping procedure conducted externally involved a fully automated real time PCR and yields an accuracy of 99.973%. Each sample was tested twice and validated against a housekeeping gene. In addition a new PCR was established in collaboration with Michael Koss (Institute of Animal Sciences, ETH Zurich) (see 2.4.2).

2.4.1 Tail samples, mouse tail tip amputation

Biopsies from mouse pups were taken during the perfusion. About 0.5 - 1.0cm of the tail tip was cut with a sharp scissor and the tissue was collected in labelled 1.5ml Eppendorf tubes. The collected specimens were stored at -20°C until analysed.

2.4.2 Establishment of multiplex PCR

2.4.2.1 DNA preparation from tissue (mouse tail tip) with isopropanol-precipitation

Material

1. Thermal shaker
2. Solubilization buffer (500µl, Tab. 4.)
3. Proteinase K (50µl) (Promega Co, Madison, USA)

} Addition of 550µl per tail tip

4. Tail salt solution (200µl per tail tip, Tab. 5.)
5. Isopropanol
6. 70% ethanol (ice cold, stored in -20°C)
7. TE (Tris-EDTA buffer) (Tab. 6.)

Method

The mouse tail tips were transferred into labelled Eppendorf tubes containing solubilization buffer plus proteinase K. The tubes were incubated at 55°C on a thermal-shaker with 950rpm followed by addition of tail salt solution for a further incubation of 30min before samples were centrifuged for 10min at 4°C (13000rpm). The supernatant was transferred into new tubes and isopropanol was added. The samples were centrifuged for another 30min at 4°C (15000rpm). The supernatant was carefully decanted and the pellet was washed by adding ice cold 70% ethanol followed by a last centrifugation step for 15min at 4°C. Finally, the supernatant was completely removed with a pipette and the pellet was air dried for about 20min before the DNA pellet was re-dissolved with TE buffer (55°C, 150rpm, 1-2h or over night at room temperature).

Table 4. Mouse tail solubilization buffer (50ml buffer)

Substance	Stock concentration	Volume [ml]	End concentration
SDS	10%	5	1%
Sodium acetate	3M	5	0.3M
EDTA	50mM	1	1mM
Tris-HCl (pH 6.8)	1M	0.5	10mM
Filled up to 50ml with aqua dest.			

Table 5. Tail salt solution (50ml solution)

Substance	Concentration [g/50ml]	End concentration [M]
NaCl	12.3	4.21
KCl	2.3	0.63
Filled up to 45ml with Tris-HCl (10mM), pH adjusted to 8.0 (HCl or NaOH), filled up to 50ml		

Table 6. TE buffer

Substance	Concentration
Tris-HCl pH 8.0	1mM
EDTA	0.1mM

2.4.2.2 DNA amplification with PCR Thermocycler (multiplex protocol)

Material

1. H_2O
2. Green PCR-Buffer (Promega Co, Madison, USA)
3. $MgCl_2$ (Promega Co.)
4. dNTP's (Promega Co.)
5. Primer Nr. 206 (10µM) ko
6. Primer Nr. 207 (10µM) ko
7. Primer Nr. 208 (10µM) wt
8. Primer Nr. 209 (10µM) wt
9. Go-Taq® Flexi DNA Polymerase (Promega Co.)
10. DNA-template

Method

Genotype-specific primers are listed in Table 7. All reagents of the mastermix (shown in Tab. 8.) were mixed and transferred to sterile 200µl tubes before 1µl DNA template was added into each tube to a total volume of 25µl. All tubes were then placed in a PCR thermocycler with the program conditions as follows (see also Tab. 9.): denaturation at 94°C for 1min followed by 40 cycles of 92°C melting for 30s, annealing at 62°C for 30s and synthesis at 72°C for 30s, followed by a final incubation for extension at 72°C for 5min. The samples were then kept at 4°C.

Table 7. Genotyping primers used

Primer	Sequence (5' - 3')	Length [mer]	Tm [°C]	Location	Product size [bp]
Primer for IAPP ko Neo					
206	cttgggtggagaggctattc	20	58.7°C/57.5	Chromosome 6	200
207	cacagctgcgcaaggaac	18	61.8°C/57.1		
Primer for IAPP wt (replaced sequence in ko)					
208	gtagcaaccctcagatggac	20	57.2°C/57.5	Chromosome 6	107
209	gaggactggaccaaggttgt	20	59.0°C/57.5		

Table 8. PCR-Master-Mix (1x) + DNA template

Volume	Substance	Concentration
14.375µl	H_2O	
5,0µl	Green PCR-Buffer (5x)	
2.0µl	$MgCl_2$ 25mM	
0,5µl	dNTP's 10mM each	0.1mM each dNTP
0,5µl	Primer Nr. 206 ko	10µM
0,5µl	Primer Nr. 207 ko	10µM
0,5µl	Primer Nr. 208 wt	10µM
0,5µl	Primer Nr. 209 wt	10µM
0,125µl	Go-TaqPolymerase 5u/µl	0.625u
1µl	DNA-template (or H_2O control)	
Total Volume of 25µl		

Table 9. PCR conditions

Cycles	Time	Temperature	Process step
1	1'	94°C	Start
40	30''	92°C	Melting
	30''	62°C	Annealing
	30''	72°C	Synthesis
1	5'	72°C	Synthesis
	∞	4°C	hold

2.4.2.3 Separation of PCR products

Horizontal electrophoresis through a 2.0% agarose gel was used to separate PCR products.

Material

1. Agarose (Agarose electrophoresis grade, #820723, MP Biomedicals, Inc., Solon, Ohio, USA)
2. Ethidiumbromid
3. DNA ladder: 100bp (Fermentas International Inc., Canada)
4. TBE buffer (buffer solution containing a mixture of Tris base, boric acid and EDTA)

Preparation of a 2.0% agarose gel

2.0g of agarose was dissolved in 100ml 1x TBE buffer (Tab. 10.) and heated in a microwave until it was completely dissolved. The solution was cooled for a few minutes and afterwards, 2µl of ethidium bromide (staining for visualization PCR products) were added and mixed without creating bubbles.

The gel was poured in an electrophoresis chamber and the chamber comb was inserted before the gel cooled completely and solidified. Bubbles were removed using a pipette tip. The chamber was filled with 1x TBE buffer to cover the gel with a layer of about 3 - 5mm. Afterwards the comb was removed.

Table 10. 1x TBE buffer

Substance	Concentration [g/10l]	End concentration [mM]
Tris-HCl pH 8.0	108	89
Boric acid	55	89
EDTA	74.4	20

Sample preparation

Because the PCR was done with Go-Taq-polymerase and Green PCR-Buffer the PCR products could directly be loaded into the gel slots, in parallel with a DNA molecular weight marker (100bp DNA Ladder) for size estimation. 12µl of each sample and the DNA marker were carefully filled in with a pipette and the electrophoresis was run at 140V for 40min until the yellow dye of the Green PCR Buffer reached the end of the gel. Representative samples were used as positive control and distilled water as negative control (ntc).

After the electrophoresis the gel was exposed to UV-light for visualization and documentation of the amplicons. The amplicons had the following expected sizes in the different genotypes:

Table 11. Expected bands

Genotype	Primers	Ampificat size
-/- knockout	206/207	200bp (neo insert)
	208/209	no product
+/- heterozygous	206/207	200bp
	208/209	107bp
+/+ wildtype	206/207	no product
	208/209	107bp (IAPP)

2.5 Statistical analysis

All data were presented as means ± SEM. Statistical significance was determined by parametric t-test of data with normal distribution (Kolmogorov-Smirnov normality test) or non-parametric Mann Whitney test using Prism Version 5.0a for Mac OS X (GraphPad Software Inc., San Diego, CA, USA). A p-value < 0.05 was considered to be statistically significant.

3 Results

3.1 Genotyping

All animals used in this study were generated from heterozygous breeding pairs. Thereby the genotype of the offspring was not known at the time of DiI implantation. We designed a multiplex PCR protocol with four primers. Figure 9. shows a representative electrophoresis agarose gel demonstrating the estimated bands. The genotypes were identical to the results obtained by the external genotyping (Transnetyx).

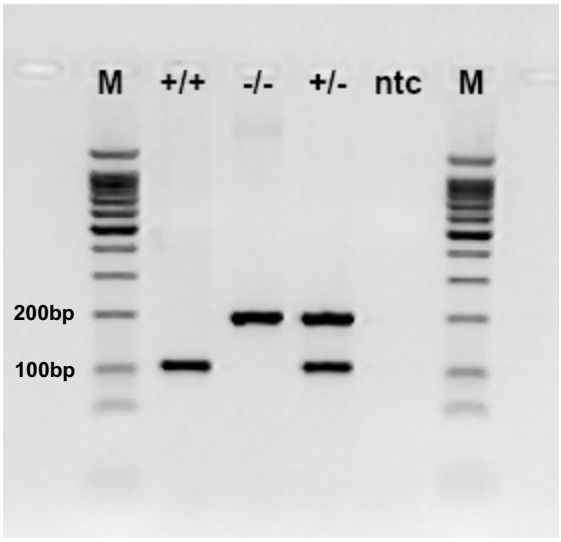

Fig. 9. Electrophoresis agarose gel showing the amplicons of the multiplex PCR. The expected bands were 107bp ($IAPP^{+/+}$), 200bp ($IAPP^{-/-}$), and 200bp/107bp ($IAPP^{+/-}$).
M = marker (100bp, 200bp), ntc = no template (neg.) control, -/- = ko $IAPP^{-/-}$, +/+ = wt $IAPP^{+/+}$, +/- = het $IAPP^{+/-}$

3.2 Neurotrophic effect of amylin

3.2.1 Fiber density in the NTS on P10 and P14

The DiI tracing experiments were conducted with amylin knockout ($IAPP^{-/-}$) mice (n=15) and their wildtype littermates ($IAPP^{+/+}$) (n=17) on day 10 or 14 after birth, respectibely. Representative implantation sites are shown in Figure 10. The diffusion fields of the tracer at the implantation sites were largely restricted to the AP.

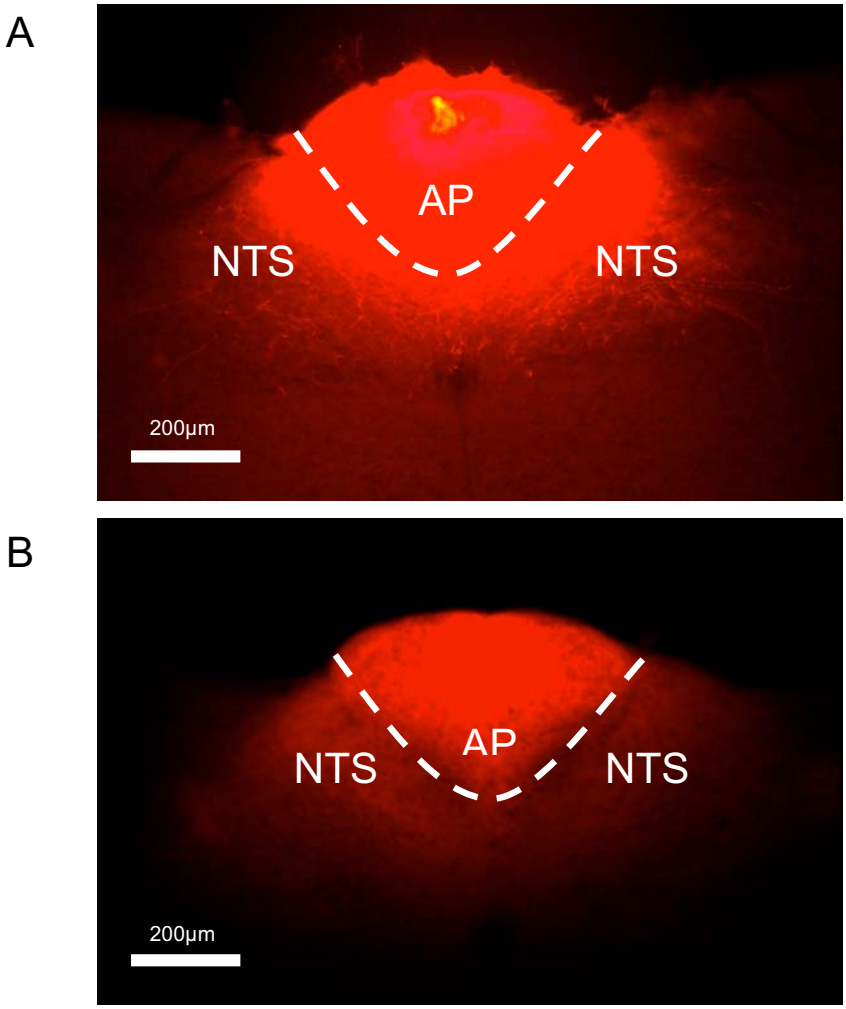

Fig. 10. Implantation site of amylin knockout and wildtype mice

A $IAPP^{+/+}$ mice, **B** $IAPP^{-/-}$ mice

AP = area postrema, NTS = nucleus of the solitary tract, dashed line = borderline of the AP

In 10 day old pups the fiber density (expressed as total fiber length in a volume of 3.4 x $10^{-3}mm^3$) in the NTS was significantly reduced in $IAPP^{-/-}$ mice compared to their wildtype littermates (males and females combined; ko: 8859 ± 2843µm vs. wt: 19769 ± 2428µm, $p < 0.01$) (Fig. 11.). P14 $IAPP^{-/-}$ mice also had lower fiber density than $IAPP^{+/+}$ littermates (male and female combined; ko: 7162 ± 3050µm vs. wt: 11470 ± 2850µm, $p = 0.3$). However this difference did not reach statistical significance (Fig. 11.). The difference in fiber density between $IAPP^{-/-}$ and $IAPP^{+/+}$ mice was more pronounced in P10 than in P14 animals (55% vs. 35%). Confocal images in Figure 12 and + 13 demonstrate the lower fiber density of P10 and P14 $IAPP^{-/-}$ mice compared to $IAPP^{+/+}$.

The fiber density of 14 day old $IAPP^{+/+}$ mice was lower compared to 10 day old $IAPP^{+/+}$ animals (P14 wt: 11470 ± 2850µm vs. P10 wt: 19770 ± 2428µm) but the difference just failed to be significant ($p = 0.051$). The fiber density of 14 day old $IAPP^{-/-}$ mice compared to 10 day old $IAPP^{-/-}$ mice was similar (P14 ko: 7162 ± 3050µm vs. P10 ko: 8859 ± 2843µm).

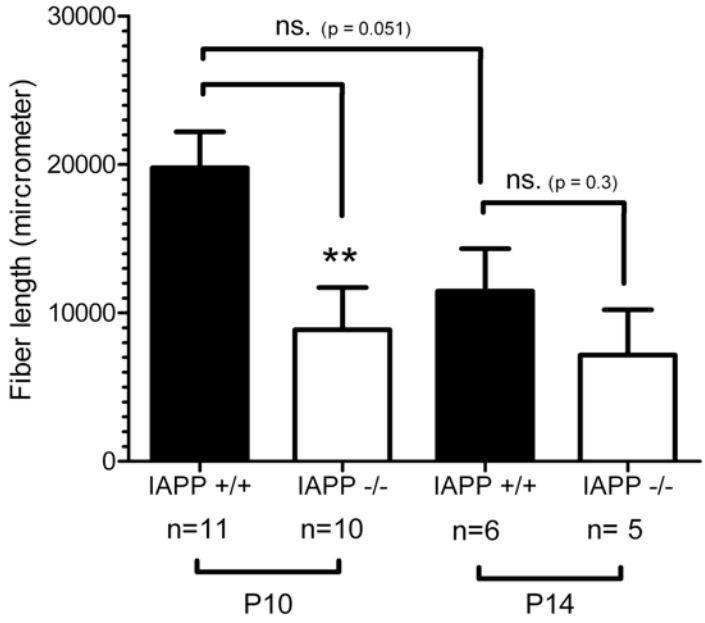

Fig. 11. Total fiber length in the NTS of P10 and P14 amylin knockout mice compared to wildtype littermates (males and females combined). The total fiber length contained in the entire volume of the image stack (3.4 x $10^{-3}mm^3$) on P10 and P14 was measured. $IAPP^{-/-}$ mice showed a significantly lower total fiber length compared to $IAPP^{+/+}$ littermates on P10. The tendency was similar on P14.

All data are expressed as mean ± SEM: **, $p < 0.01$; $IAPP^{-/-}$ vs. $IAPP^{+/+}$; ns. = not significant

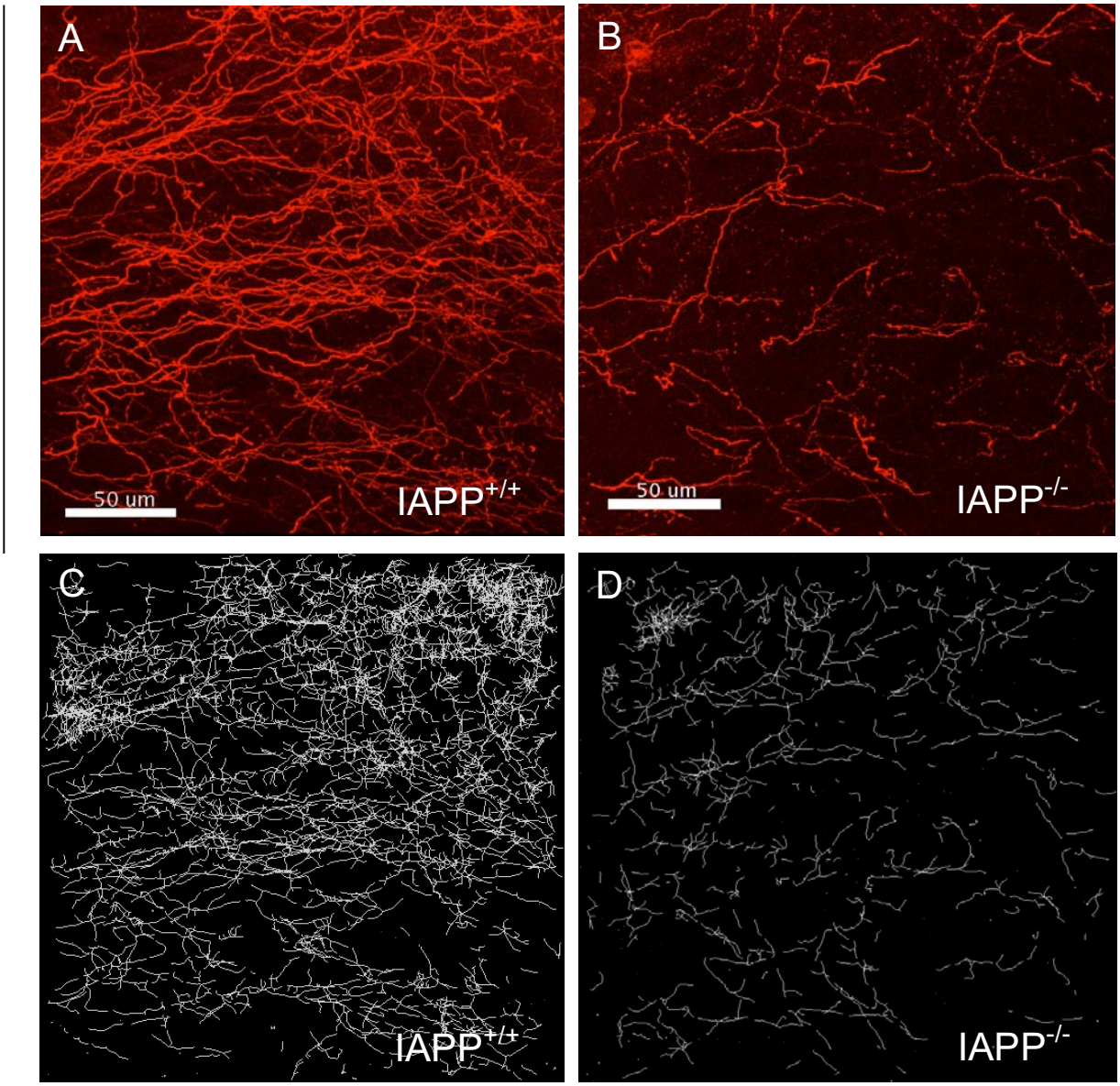

Fig. 12. Representative three-dimensional confocal image stacks and skeletonized fiber tracings (male P10 mouse).

A + B Confocal images illustrating the fiber density in the NTS of P10 $IAPP^{-/-}$ compared to $IAPP^{+/+}$ mice

C + D Fiber skeleton corresponding to the neuronal projections in A + B

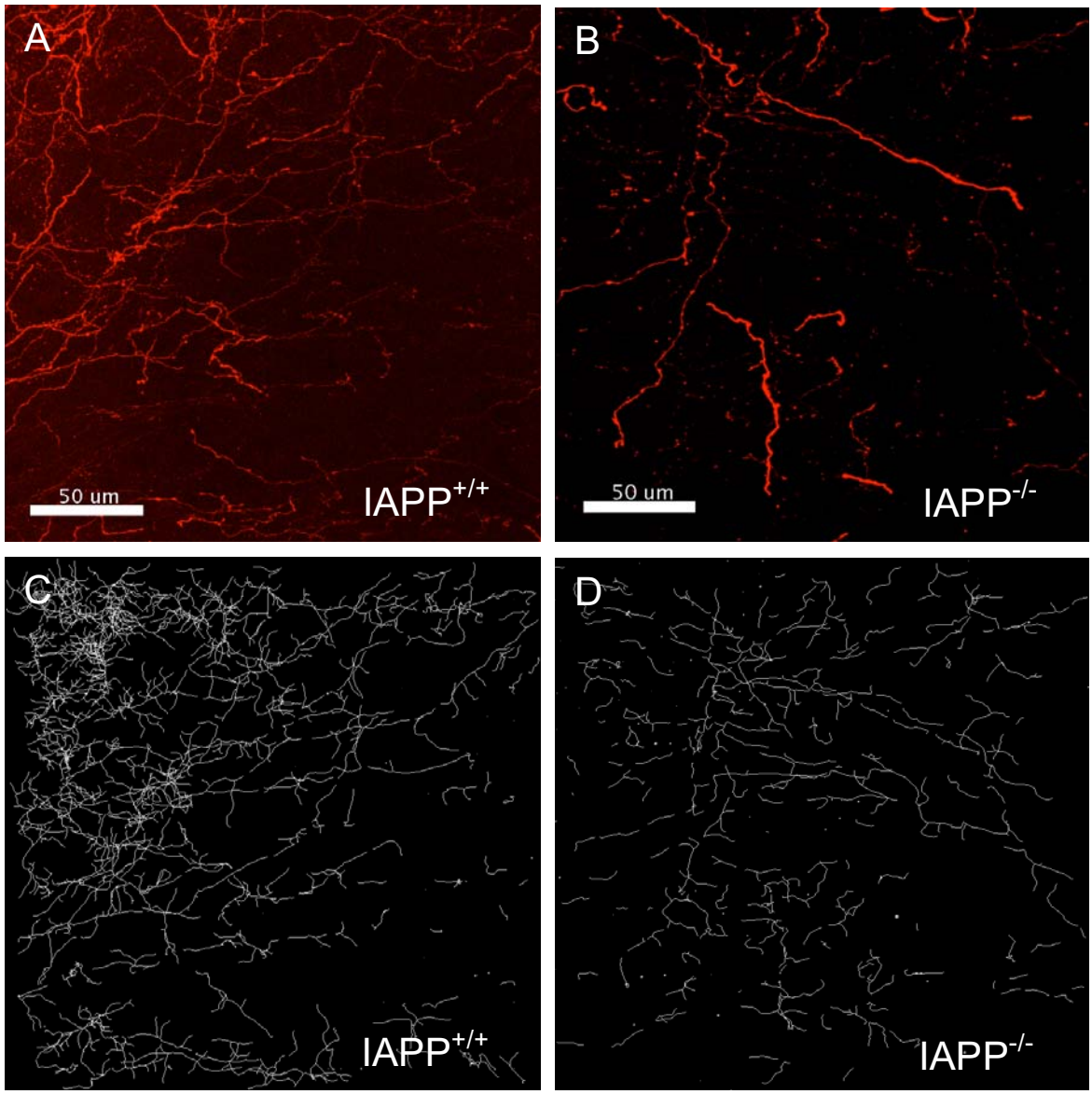

Fig. 13. Representative three-dimensional confocal image stacks and skeletonized fiber tracings (male P14 mouse).

A + B Confocal images illustrating the fiber density in the NTS of P14 $IAPP^{-/-}$ compared to $IAPP^{+/+}$ mice

C + D Fiber skeleton corresponding to the neuronal projections in A + B

3.2.2 Fiber density in the NTS of male compared to female mice on P10

To investigate, if there was a difference in AP-NTS projections between male and female animals, we conducted a gender-specific analysis. Similar to the combined data, P10 male IAPP$^{-/-}$ mice had a significantly lower fiber density than male IAPP$^{+/+}$ mice (P10 male ko: 10457 ± 3341µm vs. P10 male wt: 23162 ± 3265µm, $p < 0.05$). Female IAPP$^{-/-}$ mice also had a much lower fiber density than female IAPP$^{+/+}$ mice. However, these data were not evaluated statistically because after exclusion of unsuccessful implantations and heterozygous genotypes, the group size of the female IAPP$^{-/-}$ mice (n=2) was too small for statistical analysis.

There seemed to be a tendency of a lower fiber density in female IAPP$^{+/+}$ vs. male IAPP$^{+/+}$ mice, but this difference was statistically not significant (P10 female wt: 15698 ± 2974µm vs. P10 male wt: 23162 ± 3265µm, $p = 0.33$).

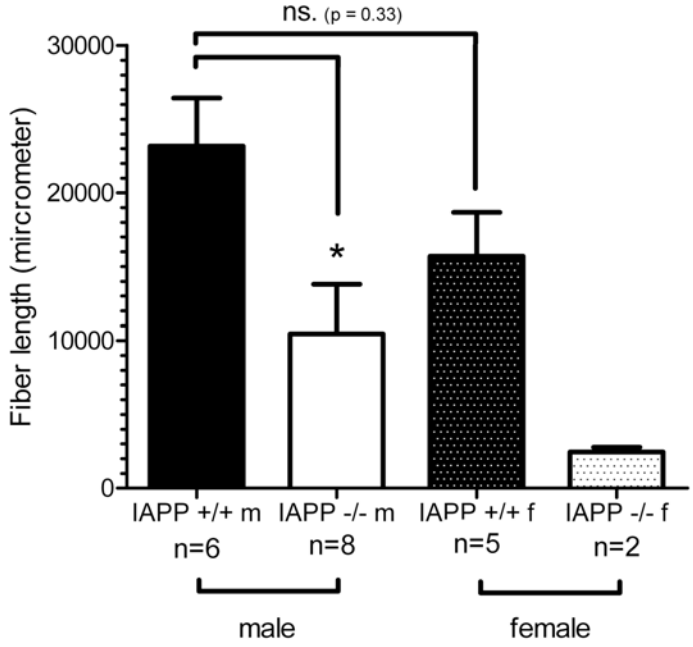

Fig. 14. Total fiber length in the NTS of male and female amylin knockout mice compared to wildtype littermates. The total fiber length contained in the entire volume of the image stack (3.4 x 10^{-3}mm^3) on P10 was measured. The fiber density in female (f) IAPP$^{+/+}$ mice was lower compared to male (m) IAPP$^{+/+}$ but the difference was not significant. Male IAPP$^{-/-}$ mice had a significantly lower fiber density compared to male IAPP$^{+/+}$ mice.

All data are expressed as mean ±SEM: *, $p < 0.05$; female IAPP$^{+/+}$ vs. male IAPP$^{+/+}$; male IAPP$^{-/-}$ vs. male IAPP$^{+/+}$; *ns. = not significant*

3.2.3 Projections outside the NTS

We observed in several DiI labelled brain slices large bilateral projections outside the NTS. The DiI dye migrated laterally from the implantation site in the AP through the NTS to other brain areas. These projections most likely correspond to AP projections described in studies using anterograde and retrograde axonal tracing techniques (van der Kooy and Koda 1983; Shapiro and Miselis 1985). The reported fibers projected to the parabrachial nucleus and demonstrated a similar bilateral distribution and pattern as the AP/NTS projections observed in our DiI labelling experiments (see Fig. 15.). We did not quantify postnatal differences in these projections between genotypes.

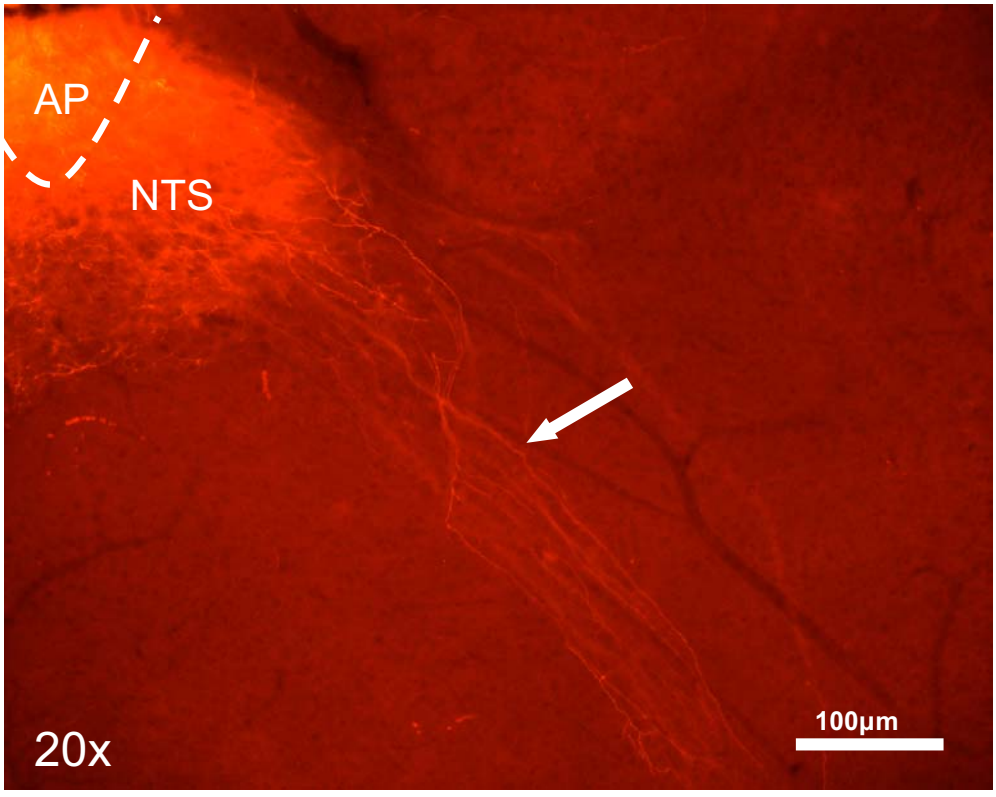

Fig. 15. DiI labelled neuronal projections (male wildtype mouse).
20X; dashed line = borderline of the AP; projections outside the NTS (with arrow)
AP = area postrema; NTS = nucleus of the solitary tract

3.3 Postnatal amylin level in BL/6 wildtype mice from P6 to P9

We took blood samples of BL/6 wildtype mice in the postnatal period (from P6 to P9) to measure the postnatal plasma amylin levels. Amylin concentrations appeared to be stable during this time period (Fig. 16.). Animals from P6 to P9 had similar plasma amylin levels compared to published values from adult mice. Of note, however, the literature data of plasma amylin levels vary depending on methodology and experimental conditions. To our knowledge the only published data in adult ad libitum fed mice came from *Leckstrom et al.*, (1999). In these studies a plasma amylin level of 14 ± 4pmol/l was reported for adult mice, measured by radioimmunoassay (Leckstrom, Lundquist et al. 1999).

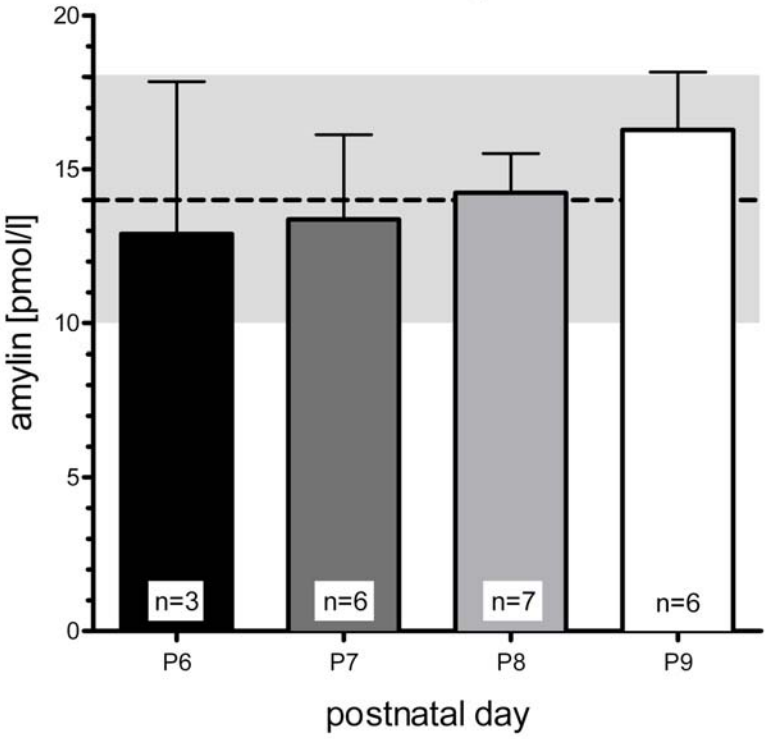

Fig. 16. Postnatal plasma amylin levels in BL/6 mice. Plasma amylin levels measured on different days after birth (from P6 to P9). Mean adult plasma amylin levels are shown as dashed line (SEM range indicated as grey area). Amylin levels from P6 to P9 were similar to those in adult animals. No change in amylin levels was observed during this time period. *P6 - P9 = postnatal days 6 – 9*

4 Discussion

This is the first study investigating a possible neurotrophic effect of amylin on the development of neuronal projections in the brain. Recent studies demonstrated a trophic effect for the lipostatic and anorectic hormone leptin in particular for projections from the ARH to the PVH, DMH, and LHA (Bouret, Draper et al. 2004a; Bouret, Draper et al. 2004b). Our hypothesis that amylin may exert a similar trophic action in the hindbrain, i.e. amylin's primary target area for its eating inhibiting effect, was put forward by studies demonstrating a trophic action of amylin in different peripheral tissues, including the kidney, the pancreas and bone tissue (Cornish, Callon et al. 1995; Harris, Cooper et al. 1997; Wookey, Tikellis et al. 1998; Cornish, Callon et al. 2001; Karlsson and Sandler 2001). On the basis of these findings, we postulated a neurotrophic effect of the anorectic hormone amylin on the development of neuronal projections from the AP to the NTS. These projections are assumed to mediate part of amylin's central nervous effects. To investigate amylin's effect on the development of these AP-NTS projections we adapted the DiI tracing approach conducted by *Bouret et al.*, (2004). We implanted crystals of the lipophilic DiI dye into the AP of amylin deficient ($IAPP^{-/-}$) mice and their wildtype (wt) littermates $IAPP^{+/+}$ on P10 and P14.

Our data provide first evidence that amylin plays a critical role for the development of AP-NTS projections because the neuronal pathways from the AP to the NTS are underdeveloped in amylin-deficient ($IAPP^{-/-}$) mice compared to their wildtype littermates. Specifically the average fiber density (expressed as total fiber length in a volume of $3.4 \times 10^{-3} mm^3$) in the NTS was significantly lower (55%) in $IAPP^{-/-}$ mice compared to $IAPP^{+/+}$ littermates on postnatal day 10. Interestingly, P14 $IAPP^{+/+}$ animals displayed a lower NTS fiber density than $IAPP^{+/+}$mice on P10 although this difference just failed to reach statistical significance. Although the fiber density of P10 and P14 $IAPP^{-/-}$ was similarly low, the difference between P14 $IAPP^{+/+}$ mice and their amylin deficient littermates was smaller than the difference observed on P10. In general the development of AP-NTS projections appeared to be disrupted both in male and female mice, although a statistical evaluation could only be conducted in male mice due to the low number of available female $IAPP^{-/-}$ mice. However, P10 $IAPP^{+/+}$ male and female animals did not significantly differ in their NTS fiber densities, although female mice tended to have lower values.

The different average fiber density between the NTS of $IAPP^{-/-}$ and $IAPP^{+/+}$ mice provides convincing evidence that amylin functions as a developmental neurotrophic factor in

the brain similar to what has been described for leptin (Bouret, Draper et al. 2004a; Bouret, Draper et al. 2004b) and for sex hormones (Rhees, Shryne et al. 1990; Ibanez, Gu et al. 2001).

In comparison to the leptin-dependent development of ARH-PVH projections, there seem to be some striking differences in the neuronal processes involved in the maturation of AP-NTS projections. One characteristic of the fiber formation from the AP appears to be existence of regressive events affecting fiber outgrowth, which is reflected by a time dependent reduction of fiber density in $IAPP^{+/+}$ pups at least between P10 and P14. Hence the maturation of projections in this brainstem area may not only involve fiber growth but also a remodelling of fibers leading to a refinement of neuronal connectivity. Such processes have also been described in other neural systems characterized in neonates using the same DiI approach. For example, fiber remodelling that is associated by reduction in fiber density has been observed in retinocollicular projections during the postnatal phase until P12 (Simon and O'Leary 1990; Simon and O'Leary 1992). It has been suggested that a refinement is achieved by removal of axons, axon segments, branches and arbors from topographically inappropriate positions. From a functional point of view an early postnatal remodelling of AP efferents appears plausible because these projections are thought to modulate or converge with enteroceptive pathways in the NTS. These pathways probably increase their stimulatory input and become operational at the onset of ingestive behaviour after birth. It is therefore tempting to speculate whether an increase in enteroceptive signalling is a necessary factor triggering the refinement of pre-developed AP-NTS projections.

In addition to the apparent remodelling processes, a further difference between the development of ARH-PVH and AP-NTS projections seems to be the onset of development itself. While the efferent ARH projections show a comparatively late postnatal development between P8 and P10, the development of AP efferents obviously takes place at an earlier postnatal or even foetal stage. In relation to what has been discussed above, the question arises whether the time range of fiber development may be associated with or influenced by the onset of ingestive behaviour. With respect to the control of food intake, newborn neonates are challenged with a sudden change of nutrient supply at birth. While prenatal nutrient supply of the foetus depends on placental transfer of maternal metabolites, the necessity to control nutrient intake emerges during postnatal development. An early development of AP-TNS connections may be an important requirement as soon as the animal is capable to control food intake. The ARH is thought to be an important target for adiposity signals involved in the long-term control of bodyweight. Apparently, the maturity of ARH-PVH projections

seems to be a less important prerequisite for the control of energy homeostasis during the early postnatal phase, which is in line with the unresponsiveness of newborn mouse pups to the anorectic action of leptin (Mistry, Swick et al. 1999).

Behavioural or functional neurophysiological studies characterizing amylin sensitivity in $IAPP^{-/-}$ mice are scarce. Thus, it remains to be determined whether the disrupted development of AP projections translates into an attenuated amylin responsiveness. There are indications that 12h food deprived amylin knockout mice show a slightly but not significantly higher food intake and an increased body weight gain than wildtype control animals (Mollet, Meier et al. 2003; Lutz 2005). On one hand these effects may be due to the lack of amylin and its anorectic action, on the other hand food intake and body weight gain may be altered as a consequence of the immature neuroanatomy of amylin deficient mice.

Future studies should characterize the time course of fiber development at earlier and later timepoints compared to the present work. It is of high interest to shed more light on the critical time window of fiber development and maturation. Furthermore, the basic question should be addressed whether amylin deficiency has an impact on the ingestive behaviour and neurophysiology in the mature adult brain. Feeding studies and immunohistological c-Fos studies characterizing the amylin responsiveness in $IAPP^{-/-}$ and $IAPP^{+/+}$ could be conducted to explore these issues.

An experimental approach to further substantiate the critical role of amylin as a neurotrophic factor may be an early postnatal amylin replacement in amylin deficient neonates. Interestingly, repeated daily leptin injection effectively rescues the disruption of ARH-PVH projection in postnatal leptin deficient *ob/ob* mice (Bouret, Draper et al. 2004b). Whether a similar amylin treatment would also reverse the attenuated fiber growth in $IAPP^{-/-}$ mice probably depends on the time range when the developing brain is sensitive to the neurotrophic action of endogenous amylin, which is still unknown. Even DiI studies characterizing NTS fiber densities in $IAPP^{-/-}$ mice at earlier developmental stages are not appropriate to identify this critical time window because genetic amylin deficiency is not a time dependent factor.

Possible indications about the critical time of amylin's neurotrophic action may be derived from alterations in circulating amylin plasma levels, which for technical reasons (limited volume of blood samples) can only be determined in mouse pups after a certain age. Unlike the postnatal profile of leptin blood values with a peak on P10 (Ahima, Prabakaran et

al. 1998), we did not detect an early postnatal amylin surge at least between P6 and P9. Amylin plasma values were relatively constant and were in the range of amylin levels measured in ad libitum fed adult mice (Leckstrom, Lundquist et al. 1999). Thus, it is conceivable that amylin might influence the brain development already before P6, but it may be experimentally difficult to assess this by earlier amylin measurements.

The present study does not rule out that amylin may act prenatally to bring about its neurotrophic effect. Our observations suggest ongoing maturation processes between P10 and P14 that may be important by amylin. Since these remodelling processes appeared to specifically affect $IAPP^{+/+}$ mice it is possible that postnatal amylin replacement may rescue this dynamic refinement. In case of a critical prenatal neurotrophic action of amylin the possibility to modulate the development of AP-NTS projections by amylin treatment of the mother seem to be limited. It is unclear whether amylin crosses the placenta in sufficient amounts to exert an influence on the embryonic brain. Studies characterizing the human ex vivo placental transfer of the amylin analogue pramlintide demonstrated a negligible passage of this peptide across placental barrier and similar results were obtained for exenatide, a synthetic 39 amino acid GLP-1 receptor agonist (Hiles, Bawdon et al. 2003). Provided that the placental transfer of amylin is similarly low this observation bears two important implications, at least for humans. First, it is unlikely that prenatal amylin treatment of the mother directly affects the embryo. Similarly, physiological or pathological changes in maternal blood amylin probably also do not influence the developmental process of the embryonic brain via a direct impact of maternal amylin. However, amylin is already expressed in the foetal period (Rindi, Terenghi et al. 1991; Mulder, Ekelund et al. 1997) giving rise to a possible neurotrophic action of foetal amylin during prenatal brain development.

Our results did not reveal a gender-specific difference in the development of AP-NTS projections although there was a tendency towards lower fiber densities in female mice, both in $IAPP^{+/+}$ and $IAPP^{-/-}$ animals. Clearly a higher sample size is required to provide further support of possible gender-specific differences. Moreover, it has to be taken into consideration that the comparison between male and female neuroanatomy may be complicated by general gender-specific differences in brain development. Given the fundamental role of sex hormones for brain development (Arnold and Gorski 1984; Toran-Allerand 1984; Rhees, Shryne et al. 1990; Ibanez, Gu et al. 2001; Simerly 2002) such differences may also exist in the NTS region which has been shown to express receptors for

sex steroids (Shughrue, Lane et al. 1997; Haywood, Simonian et al. 1999; Asarian and Geary 2007). Irrespective of a developmental influence of sex hormones on the formation of AP-NTS our data clearly point to a similar neurotrophic action of amylin in both male and female mice.

Based on the current findings the question arises whether amylin is also important for neuronal development in other brain areas and which mechanisms may mediate this action at the cellular level. A simple approach to test this may be the comparison of brain weight and volume between $IAPP^{-/-}$ and $IAPP^{+/+}$ mice, as it has been investigated for leptin deficient mice (Steppan and Swick 1999). If amylin exerted an overall effect on brain development, $IAPP^{-/-}$ may show reduced brain weight and volume. Furthermore, amylin replacement might reverse this effect. In addition specific DiI tracing studies in other brain sites are required in order to confirm a more widespread neurotrophic action of amylin in the CNS. It may be interesting to include brain areas with and without known amylin receptor expression.
With regard to the possible mechanism mediating the trophic action of amylin it is reasonable to presume that amylin receptors are involved although this assumption awaits furthers experimental validation. Interestingly, the caltitonin receptor (CTR), which forms the core component of the amylin receptor, is expressed early during ontogeny. Due to its spatiotemporal distribution throughout the brain during early embryonic brain development the CTR is thought to play a role in neuroblast migration and activation (Tolcos, Tikellis et al. 2003). In the AP of adult rats a high density of CTR is expressed (Barth, Riediger et al. 2004; Becskei, Riediger et al. 2004) together with RAMPs that are necessary for amylin affinity (Barth, Riediger et al. 2004). Whether functional amylin receptors mediate amylin's effect of neuronal growth and whether this mediation determines which brain areas are sensitive to amylin's neurotrophic action remains to be clarified.

In conclusion the present study provides convincing evidence that amylin is important for the development of neuronal projections from the AP to the NTS. Similar to the discovery of leptin's neurotrophic action, this observation strongly suggests a critical function for amylin as a developmental signal promoting the maturation of important neural brainstem pathways, possibly involved in the control of food intake and fuel homeostasis. Hence, the developing brain may be sensitive or even vulnerable to perinatal alterations in amylin levels. This supports the emerging opinion that hormonal and metabolic influences during critical stages of ontogeny lead to a programming of neuronal circuits with consequences for brain

function during adulthood. Impressive evidence for this view came from recent studies demonstrating underdeveloped neuronal hypothalamic ARH projections in the offspring of diet-induced obese rats (Bouret, Gorski et al. 2008) that in turn is also prone to leptin resistance and obesity. Interestingly, such developmental disturbances seem to increase the risk for obesity and associated metabolic disorders such as diabetes mellitus later in the life. The current study adds further support to this concept of developmental hormonal imprinting with amylin being a possible key factor.

5 Summary

Amylin is a 37 amino acid peptide which is synthesized in pancreatic beta-cells and co-secreted with insulin in response to food intake. The best investigated effects of amylin include an inhibition of food intake, glucagon secretion and gastric emptying. In vivo studies identified the area postrema (AP) of the brainstem as the primary target structure for these actions, where amylin exerts excitatory effects. The amylin-induced excitation is transmitted via neuronal projections to the nucleus of the solitary tract (NTS), which is an important relay center for signals from the AP but which also receives signals directly from the gastrointestinal tract via vagal and non-vagal afferents. Apart from its central nervous effects, amylin has been shown to act as growth factor in bone cells, pancreatic islets and the kidney where amylin leads e.g. to the proliferation of proximal tubule cells. It was the aim of the present study to explore whether amylin exerts neurotrophic effects during early brain development that may contribute to the growth of neuronal pathways originating in the AP.

Recent studies had shown that the lipostatic and anorectic hormone leptin is essential for the postnatal delevopment of neuronal projections from the hypothalamic arcuate nucleus to other hypothalamic key structures for the regulation of energy balance. Based on a similar experimental approach crystals of the lipophilic tracer DiI were implanted into the AP of postnatal amylin deficient ($IAPP^{-/-}$) mice and their wildtype littermates ($IAPP^{+/+}$).

In 10 day old neonates the average fiber density in the NTS of $IAPP^{-/-}$ mice was significantly reduced compared to $IAPP^{+/+}$ littermates. There was no obvious gender specific difference because a lower NTS fiber density was found in both male and female $IAPP^{-/-}$ mice. Interestingly, there seemed to be neuronal remodelling processes between postnatal day 10 and 14 which were reflected by a decrease in the NTS fiber density of $IAPP^{+/+}$ mice during this time period. In additional experiments we assessed the plasma amylin levels in neonates from postnatal day 6 to 9. At this stage amylin levels were similar to published values obtained from adult mice supporting the presumed role of amylin as neurotrophic factor during the early brain development.

In conclusion this study provides first evidence for a critical function of amylin as a neurotrophic factor affecting the development of important brainstem pathways involved in the control of food intake. Therefore the present findings substantiate the concept that the developing brain is imprinted by and possibly vulnerable to hormonal influences during the perinatal stage. There is cumulative evidence that such processes may have an impact on the risk to develop metabolic diseases (e.g. diabetes mellitus) and excessive body weight (obesity) later in life.

6 Zusammenfassung

Amylin ist ein Peptid aus 37 Aminosäuren und wird in den Beta-Zellen des Pankreas gebildet, aus denen es zusammen mit Insulin als Antwort auf die Nahrungsaufnahme freigesetzt wird. Die am besten untersuchten Effekte von Amylin sind eine Hemmung der Nahrungsaufnahme, der Glukagon Sekretion und der Magenentleerung. In vivo Studien konnten die im Hirnstamm gelegene Area Postrema (AP) als die primäre Zielstruktur hinsichtlich dieser Wirkungen identifizieren. Amylin induziert in der AP exzitatorische Effekte, die über neuronale Projektionen zum Nucleus tractus solitarii (NTS) übertragen werden. Dieser stellt eine wichtige Schaltstelle für Signale von der AP dar, erhält aber auch direkt Signale aus dem Gastrointestinaltrakt über vagale und nicht vagale Afferenzen. Abgesehen von seinen zentralen Effekten wirkt Amylin auch als Wachstumsfakor in Knochenzellen, im Pankreas und in der Niere, wo es z.B. die Proliferation von proximalen Tubulus Zellen stimuliert. Es war das Ziel der vorliegenden Arbeit zu untersuchen, ob Amylin neurotrophische Effekte während der frühen Entwicklung des Gehirns ausübt und somit am Wachstum von Nervenbahnen, die aus der AP entspringen, beteiligt ist.

Wie kürzlich gezeigt wurde, ist dass das lipostatische und verzehrsreduzierende Hormon Leptin für die postnatale Entwicklung von neuronalen Projektionen, die vom Nucleus arcuatus im Hypothalmus ausgehen, essentiell. Die neuronalen Verbindungen projizieren zu anderen hypothalamischen Schlüssenstrukturen, welche ihrerseits an der Regulation der Nahrungsaufnahme beteiligt sind. Basierend auf einem ähnlichen experimentellen Ansatz implantierten wir Kristalle des lipophilen Fluoreszenz-Farbstoffes DiI in die AP von postnatalen amylin defizienten Mäusen ($IAPP^{-/-}$) und deren Wildtyp-Wurfgeschwistern ($IAPP^{+/+}$).

Die durchschnittliche Faserdichte im NTS von neugeborenen 10 Tage alten $IAPP^{-/-}$ Mäusen war signifikant reduziert, verglichen mit $IAPP^{+/+}$ Wurfgeschwistern. Dabei gab es keinen geschlechtsspezifischen Unterschied, weil sowohl männliche, als auch weibliche $IAPP^{-/-}$ Mäuse eine verminderte Faserdichte im NTS aufwiesen. Interessanterweise scheinen zwischen dem postnatalem Tag 10 und Tag 14 neuronale Umbau-Prozesse zu existieren, welche durch eine Verminderung der Faserdichten im NTS von $IAPP^{+/+}$ Mäusen in diesem Zeitraum gekennzeichnet waren. In zusätzlichen Experimenten untersuchten wir den Plasma Amylin Spiegel in neugeborenen Mäusen vom postnatalen Tag 6 bis Tag 9. In dieser Phase waren die Amylin Spiegel bereits ähnlich hoch wie veröffentliche Plasma Werte von adulten

während der frühen Entwicklung des Gehirnes.

Zusammenfassend konnte durch die vorliegende Studie erstmals eine massgebliche Funktion von Amylin als neurotrophischer Faktor nachgewiesen werden. Demzufolge dürfte Amylin an der Entwicklung von wichtigen Nervenbahnen im Hirnstamm beteiligt sein, welche an der Regulation der Nahrungsaufnahme involviert sind. Die vorliegenden Ergebnisse untermauern daher ein Konzept, nach dem das sich entwickelnde Gehirn durch hormonelle Einflüsse im perinatalen Stadium geprägt wird und möglicherweise sensibel auf hormonelle Faktoren reagiert. Wie sich immer mehr abzeichnet, scheint das Risiko zur Entstehung von Stoffwechselkrankheiten (z.B. Diabetes Mellitus) und übermäßiges Körpergewicht (Fettsucht) möglicherweise von solchen Prozessen beeinflusst zu werden.

7 References

Ahima, R. S., C. Bjorbaek, et al. (1999). "Regulation of neuronal and glial proteins by leptin: implications for brain development." Endocrinology **140**(6): 2755-62.

Ahima, R. S. and S. M. Hileman (2000). "Postnatal regulation of hypothalamic neuropeptide expression by leptin: implications for energy balance and body weight regulation." Regul Pept **92**(1-3): 1-7.

Ahima, R. S., D. Prabakaran, et al. (1998). "Postnatal leptin surge and regulation of circadian rhythm of leptin by feeding. Implications for energy homeostasis and neuroendocrine function." J Clin Invest **101**(5): 1020-7.

Arnelo, U., J. Permert, et al. (1997). "Chronic low dose islet amyloid polypeptide infusion reduces food intake, but does not influence glucose metabolism, in unrestrained conscious rats: studies using a novel aortic catheterization technique." Endocrinology **138**(10): 4081-5.

Arnold, A. P. and R. A. Gorski (1984). "Gonadal steroid induction of structural sex differences in the central nervous system." Annu Rev Neurosci **7**: 413-42.

Asai, J., M. Nakazato, et al. (1990). "Regional distribution and molecular forms of rat islet amyloid polypeptide." Biochem Biophys Res Commun **169**(2): 788-95.

Asarian, L. and N. Geary (2007). "Estradiol enhances cholecystokinin-dependent lipid-induced satiation and activates estrogen receptor-alpha-expressing cells in the nucleus tractus solitarius of ovariectomized rats." Endocrinology **148**(12): 5656-66.

Bagdade, J. D., E. L. Bierman, et al. (1967). "The significance of basal insulin levels in the evaluation of the insulin response to glucose in diabetic and nondiabetic subjects." J Clin Invest **46**(10): 1549-57.

Balasubramaniam, A., V. Renugopalakrishnan, et al. (1991). "Syntheses, structures and anorectic effects of human and rat amylin." Peptides **12**(5): 919-24.

Barth, S. W., T. Riediger, et al. (2004). "Peripheral amylin activates circumventricular organs expressing calcitonin receptor a/b subtypes and receptor-activity modifying proteins in the rat." Brain Res **997**(1): 97-102.

Baskin, D. G., T. M. Hahn, et al. (1999). "Leptin sensitive neurons in the hypothalamus." Horm Metab Res **31**(5): 345-50.

Batterham, R. L., M. A. Cowley, et al. (2002). "Gut hormone PYY(3-36) physiologically inhibits food intake." Nature **418**(6898): 650-4.

Baura, G. D., D. M. Foster, et al. (1993). "Saturable transport of insulin from plasma into the central nervous system of dogs in vivo. A mechanism for regulated insulin delivery to the brain." J Clin Invest **92**(4): 1824-30.

Beaumont, K., M. A. Kenney, et al. (1993). "High affinity amylin binding sites in rat brain." Mol Pharmacol **44**(3): 493-7.

Becskei, C., T. Riediger, et al. (2004). "Immunohistochemical mapping of calcitonin receptors in the adult rat brain." Brain Res **1030**(2): 221-33.

Bhogal, R., D. M. Smith, et al. (1992). "Investigation and characterization of binding sites for islet amyloid polypeptide in rat membranes." Endocrinology **130**(2): 906-13.

Borison, H. L. (1974). "Area postrema: chemoreceptor trigger zone for vomiting--is that all?" Life Sci **14**(10): 1807-17.

Bouret, S. G., S. J. Draper, et al. (2004a). "Formation of projection pathways from the arcuate nucleus of the hypothalamus to hypothalamic regions implicated in the neural control of feeding behavior in mice." J Neurosci **24**(11): 2797-805.

Bouret, S. G., S. J. Draper, et al. (2004b). "Trophic action of leptin on hypothalamic neurons that regulate feeding." Science **304**(5667): 108-10.

Bouret, S. G., J. N. Gorski, et al. (2008). "Hypothalamic neural projections are permanently disrupted in diet-induced obese rats." Cell Metab **7**(2): 179-85.

Bouret, S. G. and R. B. Simerly (2004c). "Minireview: Leptin and development of hypothalamic feeding circuits." Endocrinology **145**(6): 2621-6.

Bouret, S. G. and R. B. Simerly (2006). "Developmental programming of hypothalamic feeding circuits." Clin Genet **70**(4): 295-301.

Bouret, S. G. and R. B. Simerly (2007). "Development of leptin-sensitive circuits." J Neuroendocrinol **19**(8): 575-82.

Butler, P. C., J. Chou, et al. (1990). "Effects of meal ingestion on plasma amylin concentration in NIDDM and nondiabetic humans." Diabetes **39**(6): 752-6.

Carlsson, P. O., E. Karlsson, et al. (2002). "Unaltered pancreatic islet blood perfusion in islet amyloid polypeptide-deficient mice." Eur J Endocrinol **146**(1): 107-12.

Carpenter, D. O. (1990). "Neural mechanisms of emesis." Can J Physiol Pharmacol **68**(2): 230-6.

Chance, W. T., A. Balasubramaniam, et al. (1992). "Tests of adipsia and conditioned taste aversion following the intrahypothalamic injection of amylin." Peptides **13**(5): 961-4.

Chance, W. T., A. Balasubramaniam, et al. (1993). "Anorexia following the systemic injection of amylin." Brain Res **607**(1-2): 185-8.

Chance, W. T., A. Balasubramaniam, et al. (1991). "Anorexia following the intrahypothalamic administration of amylin." Brain Res **539**(2): 352-4.

Christopoulos, G., G. Paxinos, et al. (1995). "Comparative distribution of receptors for amylin and the related peptides calcitonin gene related peptide and calcitonin in rat and monkey brain." Can J Physiol Pharmacol **73**(7): 1037-41.

Christopoulos, G., K. J. Perry, et al. (1999). "Multiple amylin receptors arise from receptor activity-modifying protein interaction with the calcitonin receptor gene product." Mol Pharmacol **56**(1): 235-42.

Clementi, G., A. Caruso, et al. (1996). "Amylin given by central or peripheral routes decreases gastric emptying and intestinal transit in the rat." Experientia **52**(7): 677-9.

Considine, R. V., M. K. Sinha, et al. (1996). "Serum immunoreactive-leptin concentrations in normal-weight and obese humans." N Engl J Med **334**(5): 292-5.

Cooper, G. J., A. C. Willis, et al. (1987). "Purification and characterization of a peptide from amyloid-rich pancreases of type 2 diabetic patients." Proc Natl Acad Sci U S A **84**(23): 8628-32.

Cornish, J., K. E. Callon, et al. (2001). "Effects of calcitonin, amylin, and calcitonin gene-related peptide on osteoclast development." Bone **29**(2): 162-8.

Cornish, J., K. E. Callon, et al. (1995). "Amylin stimulates osteoblast proliferation and increases mineralized bone volume in adult mice." Biochem Biophys Res Commun **207**(1): 133-9.

Dacquin, R., R. A. Davey, et al. (2004). "Amylin inhibits bone resorption while the calcitonin receptor controls bone formation in vivo." J Cell Biol **164**(4): 509-14.

Davis, J. D. and C. S. Campbell (1973). "Peripheral control of meal size in the rat. Effect of sham feeding on meal size and drinking rate." J Comp Physiol Psychol **83**(3): 379-87.

Davison, J. S. and G. D. Clarke (1988). "Mechanical properties and sensitivity to CCK of vagal gastric slowly adapting mechanoreceptors." Am J Physiol **255**(1 Pt 1): G55-61.

Denijn, M., R. A. De Weger, et al. (1992). "Islet amyloid polypeptide (IAPP) is synthesized in the islets of Langerhans. Detection of IAPP polypeptide and IAPP mRNA by combined in situ hybridization and immunohistochemistry in rat pancreas." Histochemistry **97**(1): 33-7.

Devaskar, S. U., C. Ollesch, et al. (1997). "Developmental changes in ob gene expression and circulating leptin peptide concentrations." Biochem Biophys Res Commun **238**(1): 44-7.

Edelman, S., H. Maier, et al. (2008). "Pramlintide in the treatment of diabetes mellitus." BioDrugs **22**(6): 375-86.

Edwards, G. L. and R. C. Ritter (1981). "Ablation of the area postrema causes exaggerated consumption of preferred foods in the rat." Brain Res **216**(2): 265-76.

Ekawa, K., M. Nishi, et al. (1997). "Cloning of mouse islet amyloid polypeptide gene and characterization of its promoter." J Mol Endocrinol **19**(1): 79-86.

Elmquist, J. K., C. Bjorbaek, et al. (1998). "Distributions of leptin receptor mRNA isoforms in the rat brain." J Comp Neurol **395**(4): 535-47.

Elmquist, J. K., C. F. Elias, et al. (1999). "From lesions to leptin: hypothalamic control of food intake and body weight." Neuron **22**(2): 221-32.

Fei, H., H. J. Okano, et al. (1997). "Anatomic localization of alternatively spliced leptin receptors (Ob-R) in mouse brain and other tissues." Proc Natl Acad Sci U S A **94**(13): 7001-5.

Ferrier, G. J., A. M. Pierson, et al. (1989). "Expression of the rat amylin (IAPP/DAP) gene." J Mol Endocrinol **3**(1): R1-4.

Foord, S. M. and F. H. Marshall (1999). "RAMPs: accessory proteins for seven transmembrane domain receptors." Trends Pharmacol Sci **20**(5): 184-7.

Fry, M. and A. V. Ferguson (2007). "The sensory circumventricular organs: brain targets for circulating signals controlling ingestive behavior." Physiol Behav **91**(4): 413-23.

Fujimoto, K., H. Machidori, et al. (1993). "Effect of intravenous administration of apolipoprotein A-IV on patterns of feeding, drinking and ambulatory activity of rats." Brain Res **608**(2): 233-7.

Geary, N., J. Le Sauter, et al. (1993). "Glucagon acts in the liver to control spontaneous meal size in rats." Am J Physiol **264**(1 Pt 2): R116-22.

Gebre-Medhin, S., H. Mulder, et al. (1998b). "Increased insulin secretion and glucose tolerance in mice lacking islet amyloid polypeptide (amylin)." Biochem Biophys Res Commun **250**(2): 271-7.

Gebre-Medhin, S., H. Mulder, et al. (1998a). "Reduced nociceptive behavior in islet amyloid polypeptide (amylin) knockout mice." Brain Res Mol Brain Res **63**(1): 180-3.

Gibbs, J., R. C. Young, et al. (1973). "Cholecystokinin decreases food intake in rats." J Comp Physiol Psychol **84**(3): 488-95.

Gross, P. M. (1992). "Circumventricular organ capillaries." Prog Brain Res **91**: 219-33.

Guan, X. M., J. F. Hess, et al. (1997). "Differential expression of mRNA for leptin receptor isoforms in the rat brain." Mol Cell Endocrinol **133**(1): 1-7.

Harris, P. J., M. E. Cooper, et al. (1997). "Amylin stimulates proximal tubular sodium transport and cell proliferation in the rat kidney." Am J Physiol **272**(1 Pt 2): F13-21.

Haywood, S. A., S. X. Simonian, et al. (1999). "Fluctuating estrogen and progesterone receptor expression in brainstem norepinephrine neurons through the rat estrous cycle." Endocrinology **140**(7): 3255-63.

Hiles, R. A., R. E. Bawdon, et al. (2003). "Ex vivo human placental transfer of the peptides pramlintide and exenatide (synthetic exendin-4)." Hum Exp Toxicol **22**(12): 623-8.

Hoffman, G. E., M. S. Smith, et al. (1993). "c-Fos and related immediate early gene products as markers of activity in neuroendocrine systems." Front Neuroendocrinol **14**(3): 173-213.

Hyde, T. M. and R. R. Miselis (1983). "Effects of area postrema/caudal medial nucleus of solitary tract lesions on food intake and body weight." Am J Physiol **244**(4): R577-87.

Ibanez, M. A., G. Gu, et al. (2001). "Target-dependent sexual differentiation of a limbic-hypothalamic neural pathway." J Neurosci **21**(15): 5652-9.

Ingalls, A. M., M. M. Dickie, et al. (1950). "Obese, a new mutation in the house mouse." J Hered **41**(12): 317-8.

Johnson, A. K. and P. M. Gross (1993). "Sensory circumventricular organs and brain homeostatic pathways." Faseb J **7**(8): 678-86.

Johnson, K. H., T. D. O'Brien, et al. (1988). "Immunolocalization of islet amyloid polypeptide (IAPP) in pancreatic beta cells by means of peroxidase-antiperoxidase (PAP) and protein A-gold techniques." Am J Pathol **130**(1): 1-8.

Joyner, K., G. P. Smith, et al. (1993). "Abdominal vagotomy decreases the satiating potency of CCK-8 in sham and real feeding." Am J Physiol **264**(5 Pt 2): R912-6.

Karlsson, E. and S. Sandler (2001). "Islet amyloid polypeptide promotes beta-cell proliferation in neonatal rat pancreatic islets." Diabetologia **44**(8): 1015-8.

Kesty, N. C., J. D. Roth, et al. (2008). "Hormone-based therapies in the regulation of fuel metabolism and body weight." Expert Opin Biol Ther **8**(11): 1733-47.

Kong, M. F., P. King, et al. (1997). "Infusion of pramlintide, a human amylin analogue, delays gastric emptying in men with IDDM." Diabetologia **40**(1): 82-8.

Langhans, W. (1996). "Role of the liver in the metabolic control of eating: what we know--and what we do not know." Neurosci Biobehav Rev **20**(1): 145-53.

Leckstrom, A., I. Lundquist, et al. (1999). "Islet amyloid polypeptide and insulin relationship in a longitudinal study of the genetically obese (ob/ob) mouse." Pancreas **18**(3): 266-73.

Leighton, B. and G. J. Cooper (1988). "Pancreatic amylin and calcitonin gene-related peptide cause resistance to insulin in skeletal muscle in vitro." Nature **335**(6191): 632-5.

Lorenz, D. N. and S. A. Goldman (1982). "Vagal mediation of the cholecystokinin satiety effect in rats." Physiol Behav **29**(4): 599-604.

Lotter, E. C., R. Krinsky, et al. (1981). "Somatostatin decreases food intake of rats and baboons." J Comp Physiol Psychol **95**(2): 278-87.

Lukinius, A., E. Wilander, et al. (1989). "Co-localization of islet amyloid polypeptide and insulin in the B cell secretory granules of the human pancreatic islets." Diabetologia **32**(4): 240-4.

Lutz, T. A. (2005). "Pancreatic amylin as a centrally acting satiating hormone." Curr Drug Targets **6**(2): 181-9.

Lutz, T. A. (2006). "Amylinergic control of food intake." Physiol Behav **89**(4): 465-71.

Lutz, T. A., J. Althaus, et al. (1998b). "Anorectic effect of amylin is not transmitted by capsaicin-sensitive nerve fibers." Am J Physiol **274**(6 Pt 2): R1777-82.

Lutz, T. A., E. Del Prete, et al. (1994). "Reduction of food intake in rats by intraperitoneal injection of low doses of amylin." Physiol Behav **55**(5): 891-5.

Lutz, T. A., E. Del Prete, et al. (1995). "Subdiaphragmatic vagotomy does not influence the anorectic effect of amylin." Peptides **16**(3): 457-62.

Lutz, T. A., N. Geary, et al. (1995). "Amylin decreases meal size in rats." Physiol Behav **58**(6): 1197-202.

Lutz, T. A., A. Mollet, et al. (2001a). "The anorectic effect of a chronic peripheral infusion of amylin is abolished in area postrema/nucleus of the solitary tract (AP/NTS) lesioned rats." Int J Obes Relat Metab Disord **25**(7): 1005-11.

Lutz, T. A., R. Rossi, et al. (1998c). "Amylin reduces food intake more potently than calcitonin gene-related peptide (CGRP) when injected into the lateral brain ventricle in rats." Peptides **19**(9): 1533-40.

Lutz, T. A., M. Senn, et al. (1998). "Lesion of the area postrema/nucleus of the solitary tract (AP/NTS) attenuates the anorectic effects of amylin and calcitonin gene-related peptide (CGRP) in rats." Peptides **19**(2): 309-17.

Lutz, T. A., M. Senn, et al. (1998a). "Lesion of the area postrema/nucleus of the solitary tract (AP/NTS) attenuates the anorectic effects of amylin and calcitonin gene-related peptide (CGRP) in rats." Peptides **19**(2): 309-17.

Matsuda, J., I. Yokota, et al. (1999). "Development changes in long-form leptin receptor expression and localization in rat brain." Endocrinology **140**(11): 5233-8.

Mercer, J. G., N. Hoggard, et al. (1996). "Localization of leptin receptor mRNA and the long form splice variant (Ob-Rb) in mouse hypothalamus and adjacent brain regions by in situ hybridization." FEBS Lett **387**(2-3): 113-6.

Mistry, A. M., A. Swick, et al. (1999). "Leptin alters metabolic rates before acquisition of its anorectic effect in developing neonatal mice." Am J Physiol **277**(3 Pt 2): R742-7.

Mollet, A., S. Meier, et al. (2003). "Endogenous amylin contributes to the anorectic effects of cholecystokinin and bombesin." Peptides **24**(1): 91-8.

Moore, C. X. and G. J. Cooper (1991). "Co-secretion of amylin and insulin from cultured islet beta-cells: modulation by nutrient secretagogues, islet hormones and hypoglycemic agents." Biochem Biophys Res Commun **179**(1): 1-9.

Morley, J. E., J. F. Flood, et al. (1994). "Modulation of food intake by peripherally administered amylin." Am J Physiol **267**(1 Pt 2): R178-84.

Muff, R., W. Born, et al. (2004). "Biological importance of the peptides of the calcitonin family as revealed by disruption and transfer of corresponding genes." Peptides **25**(11): 2027-38.

Muff, R., N. Buhlmann, et al. (1999). "An amylin receptor is revealed following co-transfection of a calcitonin receptor with receptor activity modifying proteins-1 or -3." Endocrinology **140**(6): 2924-7.

Mulder, H., M. Ekelund, et al. (1997). "Islet amyloid polypeptide in the gut and pancreas: localization, ontogeny and gut motility effects." Peptides **18**(6): 771-83.

Mulder, H., S. Gebre-Medhin, et al. (2000). "Islet amyloid polypeptide (amylin)-deficient mice develop a more severe form of alloxan-induced diabetes." Am J Physiol Endocrinol Metab **278**(4): E684-91.

Naslund, E., B. Barkeling, et al. (1999). "Energy intake and appetite are suppressed by glucagon-like peptide-1 (GLP-1) in obese men." Int J Obes Relat Metab Disord **23**(3): 304-11.

Nicholl, C. G., J. M. Bhatavdekar, et al. (1992). "Extra-pancreatic expression of the rat islet amyloid polypeptide (amylin) gene." J Mol Endocrinol **9**(2): 157-63.

Proulx, K., D. Richard, et al. (2002). "Leptin regulates appetite-related neuropeptides in the hypothalamus of developing rats without affecting food intake." Endocrinology **143**(12): 4683-92.

Rhees, R. W., J. E. Shryne, et al. (1990). "Termination of the hormone-sensitive period for differentiation of the sexually dimorphic nucleus of the preoptic area in male and female rats." Brain Res Dev Brain Res **52**(1-2): 17-23.

Ricardo, J. A. and E. T. Koh (1978). "Anatomical evidence of direct projections from the nucleus of the solitary tract to the hypothalamus, amygdala, and other forebrain structures in the rat." Brain Res **153**(1): 1-26.

Riediger, T., H. A. Schmid, et al. (2001). "Amylin potently activates AP neurons possibly via formation of the excitatory second messenger cGMP." Am J Physiol Regul Integr Comp Physiol **281**(6): R1833-43.

Rindi, G., G. Terenghi, et al. (1991). "Islet amyloid polypeptide in proliferating pancreatic B cells during development, hyperplasia, and neoplasia in humans and mice." Am J Pathol **138**(6): 1321-34.

Ritter, S., J. J. McGlone, et al. (1980). "Absence of lithium-induced taste aversion after area postrema lesion." Brain Res **201**(2): 501-6.

Roth, J. D., B. L. Roland, et al. (2008). "Leptin responsiveness restored by amylin agonism in diet-induced obesity: evidence from nonclinical and clinical studies." Proc Natl Acad Sci U S A **105**(20): 7257-62.

Rowland, N. E., E. C. Crews, et al. (1997). "Comparison of Fos induced in rat brain by GLP-1 and amylin." Regul Pept **71**(3): 171-4.

Rushing, P. A., R. J. Seeley, et al. (2002). "Acute 3rd-ventricular amylin infusion potently reduces food intake but does not produce aversive consequences." Peptides **23**(5): 985-8.

Samsom, M., L. A. Szarka, et al. (2000). "Pramlintide, an amylin analog, selectively delays gastric emptying: potential role of vagal inhibition." Am J Physiol Gastrointest Liver Physiol **278**(6): G946-51.

Sawchenko, P. E. (1998). "Toward a new neurobiology of energy balance, appetite, and obesity: the anatomists weigh in." J Comp Neurol **402**(4): 435-41.

Schwartz, M. W. (1997). "Regulation of appetite and body weight." Hosp Pract (Minneap) **32**(7): 109-12, 117-9.

Schwartz, M. W., E. Peskind, et al. (1996). "Cerebrospinal fluid leptin levels: relationship to plasma levels and to adiposity in humans." Nat Med **2**(5): 589-93.

Schwartz, M. W., S. C. Woods, et al. (2000). "Central nervous system control of food intake." Nature **404**(6778): 661-71.

Sexton, P. M., A. Albiston, et al. (2001). "Receptor activity modifying proteins." Cell Signal **13**(2): 73-83.

Sexton, P. M., G. Paxinos, et al. (1994). "In vitro autoradiographic localization of calcitonin binding sites in human medulla oblongata." J Comp Neurol **341**(4): 449-63.

Shapiro, R. E. and R. R. Miselis (1985). "The central neural connections of the area postrema of the rat." J Comp Neurol **234**(3): 344-64.

Shughrue, P. J., M. V. Lane, et al. (1997). "Comparative distribution of estrogen receptor-alpha and -beta mRNA in the rat central nervous system." J Comp Neurol **388**(4): 507-25.

Simerly, R. B. (2002). "Wired for reproduction: organization and development of sexually dimorphic circuits in the mammalian forebrain." Annu Rev Neurosci **25**: 507-36.

Simon, D. K. and D. D. O'Leary (1990). "Limited topographic specificity in the targeting and branching of mammalian retinal axons." Dev Biol **137**(1): 125-34.

Simon, D. K. and D. D. O'Leary (1992). "Development of topographic order in the mammalian retinocollicular projection." J Neurosci **12**(4): 1212-32.

Stein, L. J. and S. C. Woods (1982). "Gastrin releasing peptide reduces meal size in rats." Peptides **3**(5): 833-5.

Steppan, C. M. and A. G. Swick (1999). "A role for leptin in brain development." Biochem Biophys Res Commun **256**(3): 600-2.

Tolcos, M., C. Tikellis, et al. (2003). "Ontogeny of calcitonin receptor mRNA and protein in the developing central nervous system of the rat." J Comp Neurol **456**(1): 29-38.

Toran-Allerand, C. D. (1984). "Gonadal hormones and brain development: implications for the genesis of sexual differentiation." Ann N Y Acad Sci **435**: 101-11.

Tschop, M., D. L. Smiley, et al. (2000). "Ghrelin induces adiposity in rodents." Nature **407**(6806): 908-13.

Udagawa, J., T. Hatta, et al. (2000). "Expression of the long form of leptin receptor (Ob-Rb) mRNA in the brain of mouse embryos and newborn mice." Brain Res **868**(2): 251-8.

van der Kooy, D. and L. Y. Koda (1983). "Organization of the projections of a circumventricular organ: the area postrema in the rat." J Comp Neurol **219**(3): 328-38.

van der Kooy, D., L. Y. Koda, et al. (1984). "The organization of projections from the cortex, amygdala, and hypothalamus to the nucleus of the solitary tract in rat." J Comp Neurol **224**(1): 1-24.

Westermark, P., C. Wernstedt, et al. (1987a). "Islet amyloid in type 2 human diabetes mellitus and adult diabetic cats contains a novel putative polypeptide hormone." Am J Pathol **127**(3): 414-7.

Westermark, P., C. Wernstedt, et al. (1987b). "Amyloid fibrils in human insulinoma and islets of Langerhans of the diabetic cat are derived from a neuropeptide-like protein also present in normal islet cells." Proc Natl Acad Sci U S A **84**(11): 3881-5.

Westermark, P., C. Wernstedt, et al. (1986). "A novel peptide in the calcitonin gene related peptide family as an amyloid fibril protein in the endocrine pancreas." Biochem Biophys Res Commun **140**(3): 827-31.

Westermark, P., E. Wilander, et al. (1987c). "Islet amyloid polypeptide-like immunoreactivity in the islet B cells of type 2 (non-insulin-dependent) diabetic and non-diabetic individuals." Diabetologia **30**(11): 887-92.

Weyer, C., D. G. Maggs, et al. (2001). "Amylin replacement with pramlintide as an adjunct to insulin therapy in type 1 and type 2 diabetes mellitus: a physiological approach toward improved metabolic control." Curr Pharm Des **7**(14): 1353-73.

Wimalawansa, S. J. (1997). "Amylin, calcitonin gene-related peptide, calcitonin, and adrenomedullin: a peptide superfamily." Crit Rev Neurobiol **11**(2-3): 167-239.

Woods, S. C., S. C. Benoit, et al. (2004). "Clinical endocrinology and metabolism. Regulation of energy homeostasis by peripheral signals." Best Pract Res Clin Endocrinol Metab **18**(4): 497-515.

Woods, S. C., T. A. Lutz, et al. (2006). "Pancreatic signals controlling food intake; insulin, glucagon and amylin." Philos Trans R Soc Lond B Biol Sci **361**(1471): 1219-35.

Woods, S. C., R. J. Seeley, et al. (1998). "Signals that regulate food intake and energy homeostasis." Science **280**(5368): 1378-83.

Wookey, P. J., C. Tikellis, et al. (1998). "Amylin as a growth factor during fetal and postnatal development of the rat kidney." Kidney Int **53**(1): 25-30.

Wren, A. M., C. J. Small, et al. (2000). "The novel hypothalamic peptide ghrelin stimulates food intake and growth hormone secretion." Endocrinology **141**(11): 4325-8.

Young, A. A., B. R. Gedulin, et al. (1996). "Dose-responses for the slowing of gastric emptying in a rodent model by glucagon-like peptide (7-36) NH2, amylin, cholecystokinin, and other possible regulators of nutrient uptake." Metabolism **45**(1): 1-3.

Zhang, W., Y. Hu, et al. (2005). "Stimulation of neurogenesis in rat nucleus of the solitary tract by ghrelin." Peptides **26**(11): 2280-8.

Zhang, W., T. R. Lin, et al. (2004). "Ghrelin stimulates neurogenesis in the dorsal motor nucleus of the vagus." J Physiol **559**(Pt 3): 729-37.

Zhang, Y., R. Proenca, et al. (1994). "Positional cloning of the mouse obese gene and its human homologue." Nature **372**(6505): 425-32.

8 Acknowledgement

I would like to express my gratitude to everyone who supported me while working on my thesis and who gave me the possibility to complete it.

I would specially like to thank my supervisor PD Dr. Thomas Riediger for his help, support, encouragement, and patience in all the time of research work and while writing my thesis.

Further I would like to thank Prof. Dr. Thomas A. Lutz for providing me the opportunity to join his group and for all support with his expertise and helpful advices and suggestions.

A special thank to Prof. Dr. Adrian B. Hehl, Institute of Parasitology, University of Zurich, for his collaboration, effort and patience while helping me with the confocal microscope. Also many thanks go to Michael Koss, Institute of Animal Sciences, ETH Zurich, for all his work and helpful assistance with the PCR.

Thanks also to *Amylin Pharmaceuticals* for providing amylin knockout mice.

My sincere thank to Caro, Catarina, Karoline, Manuela, Melania, Mélanie, Nadine, Christian, Peter and all the people who have contributed to and helped with my thesis. Thank you for the great and pleasant atmosphere in the group.

In the end, I would like to thank my family and friends for their motivating support what helped to finish my thesis during this time, and Ranja whose encouragement also enabled me to complete this work.

9 Curriculum vitae

Name, Vorname	Hermann, Andreas
Geburtsdatum	08.11.1983
Geburtsort	Chur, GR
Nationalität	CH
Heimatort	Fläsch, GR

1990 – 1996	Primarschule Maienfeld
1996 – 2003	Gymnasium Evangelische Mittelschule Schiers (EMS)
2003	Mittelschulabschluss, Matura Schwerpunkt Biologie/ Chemie
2004 – 2009	Studium der Veterinärmedizin, Schwerpunkt biomedizinische Forschung, Universität Zürich, Schweiz
2008 – 2009	Anfertigung der Dissertation unter Leitung von PD Dr. rer. nat. Thomas Riediger am Institut für Veterinärphysiologie der Vetsuisse-Fakultät Universität Zürich (Direktor Prof. Dr. med. vet. Max Gassmann)
2009	Abschlussprüfung vet. med. an der Universität Zürich, Schweiz

Maienfeld, 03.08.2009 Andreas Hermann